Doctoral Thesis

Studies on corneal topography of normal dogs and cats:

A cross-sectional study of keratometry in Japan

犬および猫の角膜形状の解析：

日本国内飼育個体における横断的角膜曲率調査

The United Graduate School of Veterinary Science
Yamaguchi University

Minae KAWASAKI

March 2022

Studies on corneal topography of normal dogs and cats:

A cross-sectional study of keratometry in Japan

犬および猫の角膜形状の解析：

日本国内飼育個体における横断的角膜曲率調査

A Thesis Submitted to
the United Graduate School of Veterinary Science
Yamaguchi University

In Partial Fulfilment of the Requirements for the Degree
Doctor of Philosophy in Veterinary Medicine

By
Minae KAWASAKI

Supervised by
Professor Yoshiharu OKAMOTO (Chief) and
Associate Professor Norihiko ITO (Sub)

Laboratory of Veterinary Surgery
Tottori University

March 2022

TABLE OF CONTENTS

LIST OF ORIGINAL PUBLICATIONS

Parts of this thesis have been published as:

1. Kawasaki, M., Furujo, T., Kuroda, K., Azuma, K., Okamoto, Y. and Ito, N. 2020.

   Characterising keratometry in different dog breeds using an automatic handheld keratometer.

   Vet Rec. **186**: e4. doi: 10.1136/vr.105393; and

2. Kawasaki, M., Furujo, T., Azuma, K., Okamoto, Y. and Ito, N. 2021. Keratometry in normal

   cats: a cross-sectional study in Japan using an automated handheld keratometer. *J Vet Med Sci.*

   83: 1256–1262.

<u>ABBREVIATIONS</u>

CI: confidence interval

HCL: hard contact lens

LoA: limits of agreement

OCT: optical coherence tomography

Rh: radius of the horizontal corneal meridian

R_{HCL}:   base curve of a parallel-fitting HCL, or the best-fit base curve of a HCL

RhRvavg: mean radius of the horizontal and vertical corneal meridians, or mean radius of the

              corneal curvature

RKT: refractor keratometer

R_{OCT}:   mean radius of the corneal curvature measured by a handheld anterior-segment

              OCT

R_{RKT}:   mean radius of the corneal curvature measured by an automated handheld RKT

R_{US}:   mean radius of the corneal curvature measured by a B-mode US

Rv: radius of the vertical corneal meridian

R1:   radius of the minor, or the flattest, corneal meridian

R2:   radius of the major, or the steepest, corneal meridian

R1R2avg: mean radius of the minor and major corneal meridians, or mean radius of the

              corneal curvature

|Δ(R1-R2)|:   absolute difference between the radii of the minor and major corneal meridians, or

degree of corneal astigmatism

SD: standard deviation

TUVMC: Tottori University Veterinary Medical Centre

US: ultrasonography

GENERAL INTRODUCTION

Corneal topography assesses the shape of the anterior cornea. It is important for fitting contact lenses which match the power and shape of the cornea. Numerous techniques have been proposed for measurement of corneal topography such as the placido disc and a scanning slit technique from as early as 1880s [1]. More sophisticated techniques such as Scheimpflug and optical coherence tomography (OCT) systems provide an assessment of the shape of the posterior cornea as well as that of the anterior cornea. Quantification of the corneal topography helps to determine optimum contact lens specification for a cornea, which is as precise as that achieved by assessing the behaviour of hard contact lenses (HCLs) with known specifications on a cornea [1]. While many modern topography machines provide detailed information about the shape of the cornea based on a computerised quantitative assessment of the corneal surface, it poses a challenge in terms of cost especially in the field of veterinary clinical ophthalmology.

On the other hand, a keratometer, which is used for keratometry, is a simpler and more basic instrument than many modern topography machines. Keratometry measures radii of the anterior corneal curvature, which determines the power of the cornea and astigmatism [2–3]. The precision is lower with the keratometer than with modern topography machines due to the lack of the detailed measurements [1]. However, it forms an essential part of ophthalmic examinations and is routinely performed to evaluate the refractive functions of the cornea in human ophthalmology. The values of the mean corneal curvature are referred to in various clinical settings. For instance, it is mainly used in

fitting contact lenses, determining intraocular lens power, and evaluating corneal astigmatism in association with various corneal refractive surgeries during the perioperative period [3–6]. Keratometry plays an important role in providing individually tailored therapeutic interventions for quality management of vision.

Nevertheless, keratometry remains uncommon in veterinary ophthalmology, and the practical application of keratometry in animals has been limited. From a clinical perspective, there has been an increasing interest in medical and surgical interventions which modify or alter the refractivity of the cornea in animals. For example, fitting of a contact lens has been reported to correct aphakia in a dog [7] and to provide support to the corneal surface during treatment of various corneal diseases such as spontaneous chronic corneal epithelial defects in dogs, corneal sequestrum in cats and corneal ulcers in horses [8–17]. Cataract extraction surgeries, which potentially create corneal astigmatism, have become increasingly popular especially in dogs and horses over the past few decades [18]. Keratometry in veterinary patients is expected to provide veterinarians valuable information to further optimise therapeutic interventions offered to individual patients. In particular, knowledge of species- or breed-specific keratometry of dogs and cats would provide useful guidance for determining optimum contact lens specification, which, in turn, will contribute to improve safety and efficacy of therapeutic bandage contact lenses used in these patients.

Previously, several studies have documented keratometry in animals using various instruments. These studies examined dogs and cats, as well as several other species [2, 19–29]. The instruments used in these studies included ultrasonography devices, photokeratometers, manual

keratometers, and Scheimpflug keratometers. In these studies, animals, especially dogs and cats, were often placed under sedation or general anaesthesia to obtain the measurements. More recently, three studies reported the results of keratometry in dogs and cats using automated handheld keratometers [22, 26, 30]. However, details of corneal topography and keratometry in dogs and cats of varied signalment remains scarce. Comparative analysis of keratometry obtained with different devices are also limited in animals.

Therefore, in this study, I investigated corneal topography and keratometry of normal dogs and cats using laboratory and domestic populations. While the primary focus of the study was to characterise the corneal curvature and the corneal astigmatism of dogs and cats of varied signalment which are popular in Japan in association with their signalment, the study also explored applicability, interchangeability, and precision of the measurements obtained with different techniques using laboratory beagles and mixed-breed cats. The studies were designed to partially fill the current knowledge gap around corneal topography and keratometry of normal dogs and cats, and to provide some guidance as to optimum contact lens specification for dogs and cats which are popular in Japan.

This dissertation describes studies on corneal topography and keratometry in normal dogs and cats with the following specific objectives:

1. To evaluate applicability of an automated handheld refractor keratometer (RKT) and a handheld anterior-segment OCT in awake dogs;

2. To evaluate interchangeability of the measurements obtained with three different techniques: an automated handheld RKT, a handheld anterior-segment OCT, and a B-mode

ultrasonography (US);

3. To evaluate corneal topography of dogs and cats using HCLs and to assess its association with the measurements obtained by an automated handheld RKT;

4. To describe the corneal curvature radius and the corneal astigmatism in different dog breeds using an automated handheld RKT, and to evaluate inter-breed and intra-breed variations of these measurements; and

5. To describe the corneal curvature radius and the corneal astigmatism of cats using an automated handheld RKT, and to evaluate their associations with signalment.

CHAPTER 1

Evaluating applicability of an automated handheld keratometer and optical coherence tomography in keratometry in awake dogs

1.1 Abstract

Keratometry was performed in six laboratory beagles using an automated handheld RKT and a handheld anterior-segment OCT to evaluate their applicability in awake dogs. Keratometry was conducted three times on both eyes: once with sedation (SED) and twice without sedation (AW−1 and AW−2). SED and AW−1 were performed on the same day, and AW−2 on another day. The measurements were compared between SED and AW−1 and between AW−1 and AW−2 using Wilcoxon signed-rank tests and Bland-Altman analyses, which generally showed good agreement between the sessions with both RKT and OCT. The results indicated that both devices can be used for keratometry in awake dogs without causing clinically significant variations in the measurements.

1.2 Introduction

Keratometry is the measurement of the corneal curvature and it determines the power of the cornea and astigmatism (Figure 1-1a) [2–3]. It is acquired manually or automatically by using variety of instruments which include keratometers, IOL Master, and corneal topography devices. Anterior-segment OCT is a more sophisticated and powerful tool to evaluate detailed *in-vivo* structure

of the anterior segment of the eye. It can also provide objective and quantifiable descriptions of the corneal curvature through taking high resolution images with no physical contact to the eye.

In human ophthalmology, both keratometer and anterior-segment OCT are routinely utilised for detailed examination of the cornea. It is an essential tool to achieve individually tailored therapeutic interventions for management of vision such as contact lens fitting, determination of intraocular lens power, and pre- and post-surgical evaluations of corneal astigmatism [3–6]. As such, there have been numerous studies reported on keratometry in humans [31–35]. On the other hand, examination of the cornea in veterinary ophthalmology has largely been dependent on a slit lamp and ultrasonography. Both keratometer and anterior-segment OCT are rarely available in veterinary practices, hence keratometry remains uncommon in veterinary patients.

Nevertheless, there are several studies which evaluated keratometry of dogs and cats using manual or automated keratometers [22–26, 30]. Most of these studies were conducted on animals under sedation or general anaesthesia in order to obtain reliable measurements. This is because the use of a manual keratometer is not feasible in conscious animals due to the lack of active cooperation during the measurement. More recently, an automated handheld keratometer has become available for keratometry. One of the major advantages of an automated keratometer is its ability to measure corneal curvatures rapidly and consecutively within a few seconds [3, 31–33]. It has proven useful in human paediatric and elderly patients who have difficulties in maintaining visual fixation when sitting upright [31–32, 34–35]. The instrument is expected to be also useful in veterinary patients. However, its applicability in conscious dogs has not yet been evaluated widely except one study, which

demonstrated comparable results between the measurements obtained awake and under general anaesthesia [30].

Imaging of the anterior segment of canine and feline eyes using OCT systems is a relatively new field of study in veterinary ophthalmology. The use of anterior-segment OCT is most frequently described in the studies on corneal pachymetry in dogs and other species [36–44]. Several other studies also described its use in examinations of corneal pathologies in dogs and cats [45] and in the studies on anterior segment morphometry of various species [46–47]. However, there is no study which evaluated keratometry in dogs using OCT systems.

Therefore, this study aimed to evaluate applicability of an automated handheld RKT and a handheld anterior-segment OCT in keratometry in awake dogs by comparing between the measurements obtained under sedation and those taken awake on the same day, and between those obtained awake on two different days.

1.3   Materials and Methods

Animals

A total of 12 corneas from six beagles owned by the Faculty of Agriculture at Tottori University were examined for keratometry three times over two separate days: once with sedation (SED) and twice without sedation (AW−1 and AW−2). The measuring sessions of SED and AW−1 were performed on the same day, with AW−1 immediately followed by SED. AW−2 was performed on another day, with more than one week apart from the day of the other sessions. For SED, the dogs

were treated with midazolam (0.2–0.4 mg/kg, IV) and medetomidine (0.01–0.02 mg/kg, IV) in order

to achieve visual fixation during the measurement. An artificial tear preparation containing 0.1%

sodium hyaluronate (Hyalein® Mini, Santen, Osaka, Japan) was applied to the eyes regularly in order

to prevent desiccation of the cornea during the measurements under sedation. All dogs were

determined clinically normal following thorough physical and ophthalmic examinations, and did not

have history of ocular diseases prior to enrolment in the study. All aspects of the study were approved

by the Animal Research Committee of Tottori University (permission No.: h29–T041).

Instruments

An automated handheld RKT, HandyRef-K (Nidek, Gamagoori, Japan), was used to perform

the keratometry examinations (Figure 1-1b, c). While the instrument was equipped with both

refractometer and keratometer functions, refractometer function was turned off and only keratometer

function was utilised. During examinations, the instrument projects the mire ring image of known

parameter onto the cornea. The corneal curvature of the central 3.0–4.0 mm diameter is measured

according to the size and shape of the mire ring image reflected on the anterior surface of the cornea

(Figure 1-1d, e). The calculation is done automatically and the radii of the minor (R1) and major (R2)

corneal meridians and the mean of the two meridians (R1R2avg) are generated in both millimetre and

dioptre units. Multiple measurements are automatically taken consecutively within a few seconds, and

they are accumulated within the device for each measurement session. A representative value for each

of these parameters is also generated from the set of consecutive measurements taken in each session

(Figure 1-1f). These values are automatically drawn by the device according to the functions pre-set

by the manufacturer. For the purpose of this study, the instrument was set to accumulate a maximum of 10 consecutive measurements in each session. The measurements were expressed in millimetres, and the scale interval was set to 0.01 mm.

A handheld swept-source anterior-segment OCT system (IVS–2000, Santec, Komaki, Japan) was used to image the cornea (Figure 1-1g). The system contains a super-luminescent light-emitting diode that delivers light at a wavelength of 1310 nm. It has an axial resolution of 12 μm in air, a maximum imaging depth of 3.5 mm in air, and scanning speed of 100,000 lines/sec. The system can perform a linear scan, and the scanning axis can be set at any angle between 0º and 360º. Sequential images obtained by each scan are recorded as a movie, and two-dimensional still images can be captured from the movie using a software accompanied to the system (Inner Vision, Santec, Komaki, Japan). Additionally, per-pixel luminance data of the images can be exported to excel format for analyses.

Procedures

The dogs were positioned in sternal recumbency on an examination table. The head of the dog was held upright so that the muzzle pointed forward and was parallel to the floor. The measurements of the anterior corneal curvature radius were made on both eyes in each dog using RKT and OCT in each session. The measurements were completed one after another with or without a short break in between depending on the dog's temperament. All measurements were taken by a single examiner.

With the RKT, the instrument was held in front of the eye so that the centre of the cornea

matched the centre of the reference ring image displayed on the device screen (Figure 1-1c). The measurement was taken repeatedly to obtain at least three readings and up to 10 stable readings on each eye.

With the OCT, a handheld probe was aligned in front of the eye and the cornea was scanned in two planes consecutively by setting the scanning axis at 90º (vertical) and 0º (horizontal) (Figure 1-1h). From the sequential images recorded in each plane, images that captured the corneal apex near the centre of the frame and the largest possible diameter of the cornea within the frame were selected (Figure 1-1i). Per-pixel luminance data of the selected images were displayed on a Microsoft Excel 2013 spreadsheet (Microsoft, Redmond, WA, US) and used to calculate the radii of the corneal curvature.

The measurements with the OCT were obtained manually using a method modified from that described previously (Figure 1-1j) [2]. Briefly, three points were plotted along the anterior surface of the cornea, one at the corneal apex and the other two at a given distance from the corneal apex. The coordinates of each points were determined based on position data of pixels. Using these coordinates, equations of perpendicular bisectors of the two adjacent points and the coordinates of the point of intersection of the two bisectors were calculated. The latter represented the centre of the corneal curvature. Thus, the distance from the corneal surface to this point represents the radius of the corneal curvature at the given central corneal diameter, which is calculated based on the equation of a circle. The radii of the corneal curvature were calculated at the central corneal diameters of 4, 6, 8, and 10 mm (Figure 1-1k). At least two measurements were taken on each image for each given central

corneal diameter. The average of these measurements obtained from vertical (Rv) and horizontal (Rh) images was considered as the mean radius of the corneal curvature (RhRvavg) of a given corneal diameter.

Statistical Analyses

Statistical analyses were conducted using the free software R version 3.4.1 (The R Foundation, Vienna, Austria). Wilcoxon signed-rank tests were performed to evaluate the differences between the measurements of the right and left eyes obtained by RKT and OCT, respectively. Since no statistical differences were noted between these measurements, the measurements from pairs of right and left eyes were combined to give the mean keratometric value for each animal and it was used in the subsequent analyses. The measurements obtained by the same instrument at two different sessions, namely between SED and AW−1 and between AW−1 and AW−2, were compared using Wilcoxon signed-rank tests. Bland-Altman analyses, which plot the differences of the measurements between two sessions against their mean, were used to illustrate agreement between the sessions, respectively [48]. The 95% limits of agreement (LoA) were defined as the mean±1.96 standard deviation (SD) of the difference between the sessions. For all tests mentioned above, where applicable, $P<0.05$ was considered statistically significant. The data were reported as medians and range (minimum–maximum), unless otherwise indicated.

1.4 Results

The dogs evaluated in this study included two males and four females. Their median age and

bodyweight were 6 years (1–10) and 9.3 kg (7.5–10.5). The differences of the measurements between the right and left eyes were not significant statistically for both RKT and OCT, with the median differences of 0.15 mm (0.00–0.65, P=0.64) and 0.09–0.11 mm (0.00–0.72, P=0.64), respectively.

The measurements of six beagles obtained by RKT and OCT in the three measuring sessions are shown in Figure 1-2. The median values of R1R2avg were 8.96 mm (8.24–9.71) for SED, 9.00 mm (8.65–9.11) for AW–1, and 9.11 mm (8.50–9.18) for AW–2. Those of RhRvavg were 7.94 mm (7.44–8.36), 7.82 mm (7.59–8.00), and 7.77 mm (7.50–8.05), respectively, when measured at 4 mm diameter; 8.40 mm (8.20–8.83), 8.44 mm (8.17–8.71), and 8.37 mm (8.03–8.49), respectively, when measured at 6 mm diameter; 8.85 mm (8.56–9.04), 8.78 mm (8.32–8.91), and 8.61 mm (8.20–8.73), respectively, when measured at 8 mm diameter; and 9.11 mm (8.78–9.24), 8.93 mm (8.44–9.08), and 8.80 mm (8.36–8.93), respectively, when measured at 10 mm diameter.

Table 1-1 summarises the differences in the keratometric values obtained in the three measuring sessions using RKT and OCT, together with P-values determined by Wilcoxon signed-rank tests and the 95% LoA according to Bland-Altman analyses. The median differences of R1R2avg were 0.02 mm (-0.41–0.61) when compared between the values obtained on the same day with and without sedation ($\Delta(R_{SED}\text{-}R_{AW\text{-}1})$), and -0.06 mm (-0.29–0.17) when compared between those obtained awake on two different days ($\Delta(R_{AW\text{-}1}\text{-}R_{AW\text{-}2})$). No significant difference was noted in all measured variables when the measurements with RKT were compared (P=0.56–0.84).

When the measurements with OCT were compared, the median values of $\Delta(R_{SED}\text{-}R_{AW\text{-}1})$ ranged from -0.06 to 0.31 mm depending on the diameter of measurements. The differences were not

significant in most variables (P=0.06–1.0). The only exception was those measured at 10 mm diameter in the vertical corneal meridian (P=0.04). The median values of $\Delta(R_{AW-1}-R_{AW-2})$ ranged from 0.08 to 0.25 mm depending on the diameter of measurements. Statistically significant differences were noted in RhRvavg measured at 8 and 10 mm diameters (P=0.03).

Figure 1-3 and 1-4 show Bland-Altman plots of the mean radius of the corneal curvature measured by RKT and OCT comparing between SED and AW–1 and between AW–1 and AW–2, respectively. All measurements fell within the range of 95% LoA regardless of the techniques and the central corneal diameter of the measurements.

1.5   Discussion

The results of this study revealed generally good agreement between the measurements obtained under sedation and awake on the same day and between those obtained awake on two different days, as far as the same instruments were used at both sessions. In general, the differences greater than 0.55 dioptres, which is equal to approximately 0.15 mm, are considered clinically significant [49]. While the present results found statistically significant differences between some measurements, most of them were of little significance clinically. This is especially true when the measurements were obtained awake and the mean of the two meridians, rather than the measurement of the individual meridians, were considered.

Previously, there is only one study which compared the measurements obtained under general anaesthesia and awake using two automated handheld keratometers in eight beagles [30]. The

reported differences between the measurements with and without general anaesthesia ranged from 0.03 to 0.14 mm depending on the measuring meridians and the devices used. The results were in accordance with the present results noted with RKT and had little clinical significance. These results suggest that sedation or general anaesthesia, although they were utilised conventionally in the past studies, be not necessary to obtain reasonably reliable corneal curvature measurements when automated handheld keratometers are used. The results also indicate that measurement errors which can potentially result from examiner's hand- or animal's eye-movement are not a major concern any more as it can take multiple measurements successively within a few seconds.

Furthermore, it has been reported that application of artificial tears during the corneal curvature measurement with an automated keratometer affects accuracy of the measurements in humans [50]. An automated keratometer is sensitive to alteration of the corneal refractivity as it relies its measurement on detection of the mire ring image which is refracted upon the corneal surface. The present study revealed slightly greater variabilities between the measurements obtained under sedation and those obtained awake on the same day than between those obtained awake on two different days. This may be associated with application of artificial tears during the measurements under sedation due to decreased normal tear production. Sedation makes it easier to align the eye for measurement, thus minimising errors associated with eye movement. However, the results, in fact, suggested that keratometry in dogs be better performed awake rather than under sedation when the automated keratometer is utilised.

Application of an OCT in keratometry in dogs has not been evaluated previously. Since this

is the first study of its kind in dogs, the results cannot be compared with other studies. The comparable results observed across the measuring sessions using the OCT system was similar to the results noted with the RKT. On the other hand, differences and variabilities between the measurements using the OCT tended to be slightly greater than those noted with the RKT, with a few exceptions. They were also greater when the measurements were taken at smaller central corneal diameters. These errors may partly be associated with measurement technique which involved some subjective decisions such as selection of two-dimensional images and location of the corneal apex. Although the differences and variabilities remain at clinically acceptable levels, errors attributable to an examiner as well as additional time and efforts required to obtain the measurements could become limiting factors for adopting the OCT in keratometry in dogs. Nonetheless, the present results supported feasibility of keratometry in awake dogs using the OCT system without the aid of sedation.

There are several limitations associated with this study, which include small sample size and single breed of dogs being examined. The present study involved only laboratory beagles, which tended to have good temperament and were well acclimated to handling prior to the enrolment. This may not always be the case for general dog population which are seen at veterinary practices. Thus, it is possible that sedation may be necessary in some cases. While varying ocular and facial morphologies seen among different dog breeds may potentially have impact on ease and accuracy of the examinations, it could not be assessed in the present study due to the lack of breed variations. Further studies involving a larger number of dogs with varied signalment would be useful to address these limitations. The present study employed a single trained examiner to obtain all of the

measurements. The study design was effective to minimise errors associated with the examiner, yet, at the same time, it limited evaluation of inter-examiner variabilities associated with the techniques. Additional studies involving multiple examiners would be useful to validate feasibility of the techniques further.

In summary, the present study demonstrated that both the automated handheld RKT and the handheld anterior-segment OCT system can be used for keratometry in awake dogs with reasonably good reproducibility, as far as the same device is used at every measuring sessions. Sedation or general anaesthesia are not necessary to obtain stable measurements with both devices. In fact, it appeared better to avoid such treatment as far as feasible in order to minimise variabilities of the measurements especially with the automated RKT. Considering some practical aspects such as ease of handling and expertise for measurements, and speed and objectiveness of the measurements, the automated handheld RKT would be a more convenient option over the OCT system when the dog has normal corneal surface. However, when the cornea is affected with some pathologies such as corneal ulcers, chronic keratitis and keratoconjunctivitis sicca, the OCT system would be the choice as alteration of the corneal surface refractivity adversely affects the keratometry readings. In the clinical setting, it is important to understand the advantages and disadvantages of each device and choose an appropriate device depending on corneal surface conditions.

1.6 Tables and Figures

Table 1-1. Differences in the keratometric values obtained in three measuring sessions using an automated handheld refractor keratometer (RKT) and a handheld anterior-segment optical coherence tomography (OCT) (n=6 dogs). The data were compared between those measured with and without sedation taken on the same day ($\Delta(R_{SED}-R_{AW-1})$), and between those measured awake on two different days ($\Delta(R_{AW-1}-R_{AW-2})$). The data were expressed in mm, where applicable. P-values were determined by Wilcoxon signed-rank tests. The 95% limits of agreement (LoA) were calculated as the mean±1.96SD of the difference according to Bland-Altman analyses.

| | $\Delta (R_{SED}-R_{AW-1})$ | | | | $\Delta (R_{AW-1}-R_{AW-2})$ | | | |
	Median (Minimum, Maximum)	P	95% LoA Lower	Upper	Median (Minimum, Maximum)	P	95% LoA Lower	Upper
RKT								
R1	0.10 (-0.31, 0.69)	0.56	-0.52	0.80	-0.06 (-0.37, 0.26)	0.69	-0.50	0.42
R2	-0.08 (-0.51, 0.52)	0.56	-0.68	0.61	0.01 (-0.20, 0.14)	0.84	-0.29	0.23
R1R2avg	0.02 (-0.41, 0.61)	0.69	-0.60	0.70	-0.06 (-0.29, 0.17)	0.84	-0.38	0.31
OCT Φ4 mm								
Rh	-0.06 (-0.77, 0.93)	0.84	-1.21	1.16	0.12 (-0.12, 0.45)	0.16	-0.27	0.57
Rv	0.17 (-0.32, 0.91)	0.44	-0.70	1.14	0.08 (-0.72, 0.36)	1.00	-0.89	0.75
RhRvavg	0.07 (-0.46, 0.73)	0.56	-0.84	1.03	0.12 (-0.42, 0.40)	0.84	-0.54	0.62
OCT Φ6 mm								
Rh	-0.01 (-0.52, 0.15)	0.56	-0.66	0.40	0.19 (-0.06, 0.63)	0.06	-0.21	0.66
Rv	0.16 (-0.10, 0.71)	0.16	-0.32	0.75	0.14 (-0.53, 0.32)	0.84	-0.67	0.70
RhRvavg	0.08 (-0.26, 0.37)	0.84	-0.38	0.47	0.16 (-0.19, 0.39)	0.31	-0.30	0.54
OCT Φ8 mm								
Rh	-0.02 (-0.31, 0.45)	1.00	-0.56	0.60	0.22 (-0.07, 0.38)	0.06	-0.09	0.48
Rv	0.27 (-0.03, 0.45)	0.06	-0.10	0.60	0.10 (-0.19, 0.31)	0.31	-0.28	0.44
RhRvavg	0.17 (-0.06, 0.24)	0.06	-0.09	0.37	0.14 (0.02, 0.24)	0.03	-0.02	0.30
OCT Φ10 mm								
Rh	-0.03 (-0.34, 0.49)	0.84	-0.58	0.70	0.25 (-0.19, 0.29)	0.09	-0.20	0.52
Rv	0.31 (0.10, 0.44)	0.04	0.00	0.53	0.12 (-0.16, 0.35)	0.22	-0.26	0.46
RhRvavg	0.17 (-0.12, 0.37)	0.09	-0.17	0.50	0.10 (0.04, 0.25)	0.03	-0.04	0.31

R1=radius of the minor corneal meridian; R2=radius of the major corneal meridian; R1R2avg=mean of R1 and R2; Rh=radius of the horizontal corneal meridian; Rv=radius of the vertical corneal meridian; RhRvavg=mean of Rh and Rv; Φ=the central corneal diameter at which the measurements were obtained with OCT.
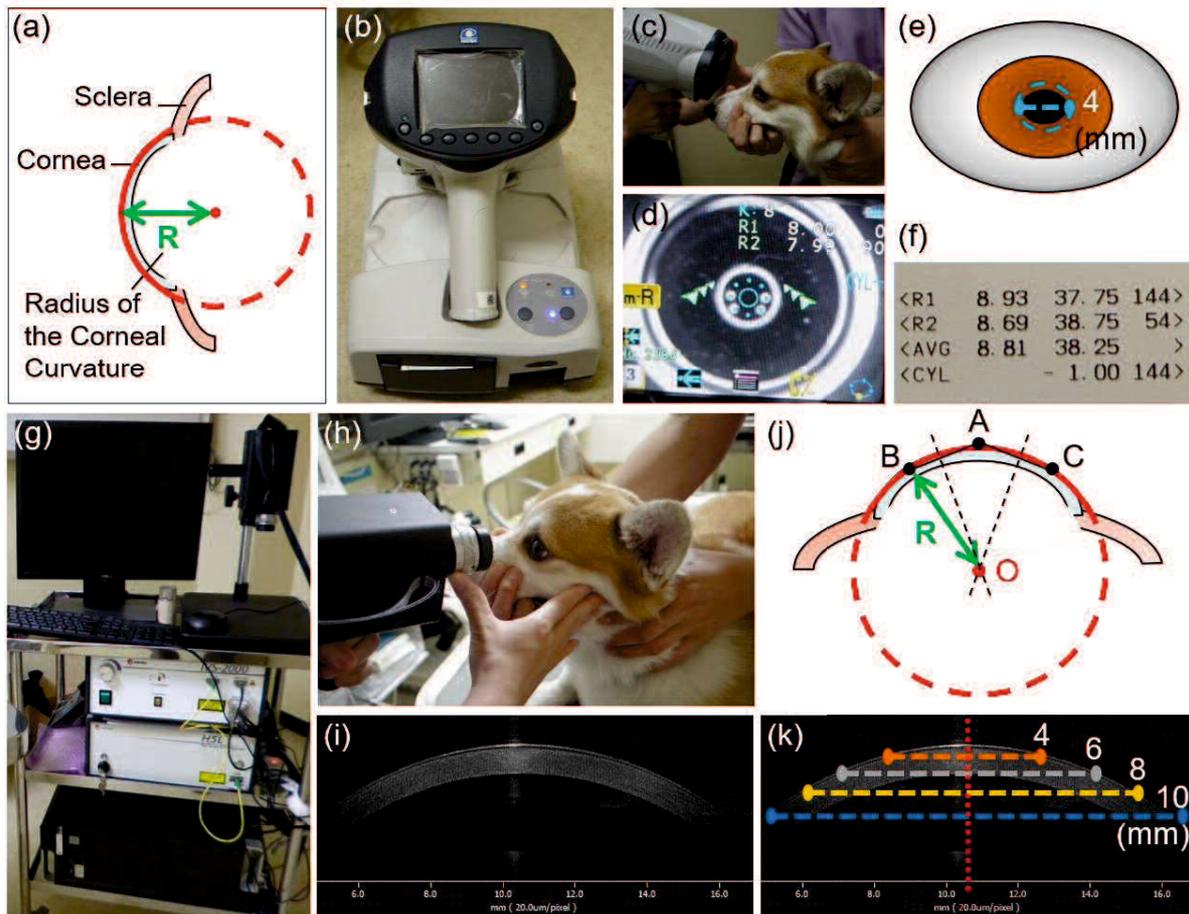
Figure 1-1. (a) A schematic diagram showing radius of the corneal curvature measured during keratometry. (b) The automated handheld refractor keratometer (RKT) used in this study. (c) Keratometry examination using the RKT. (d) Device screen of the RKT. (e) A schematic diagram illustrating the central corneal diameter at which the measurements were obtained by RKT. (f) An example of outcome data obtained by RKT. (g) The anterior-segment optical coherence tomography (OCT) system used in this study. (h) Corneal scan using the OCT. (i) A representative image of a corneal scan obtained by OCT. (j) A schematic diagram illustrating the measurement technique. Point A represents the corneal apex. Point B and C represent the points located at a given distance from the corneal apex. Dashed lines represent the perpendicular bisectors of the line AB and AC, respectively. Point O represents the point of intersection of the two bisectors, which represents the centre of the corneal curvature. Distance R represents the radius of the corneal curvature. (k) A schematic diagram illustrating the central corneal diameters at which the measurements were obtained by OCT using the technique illustrated in (j).
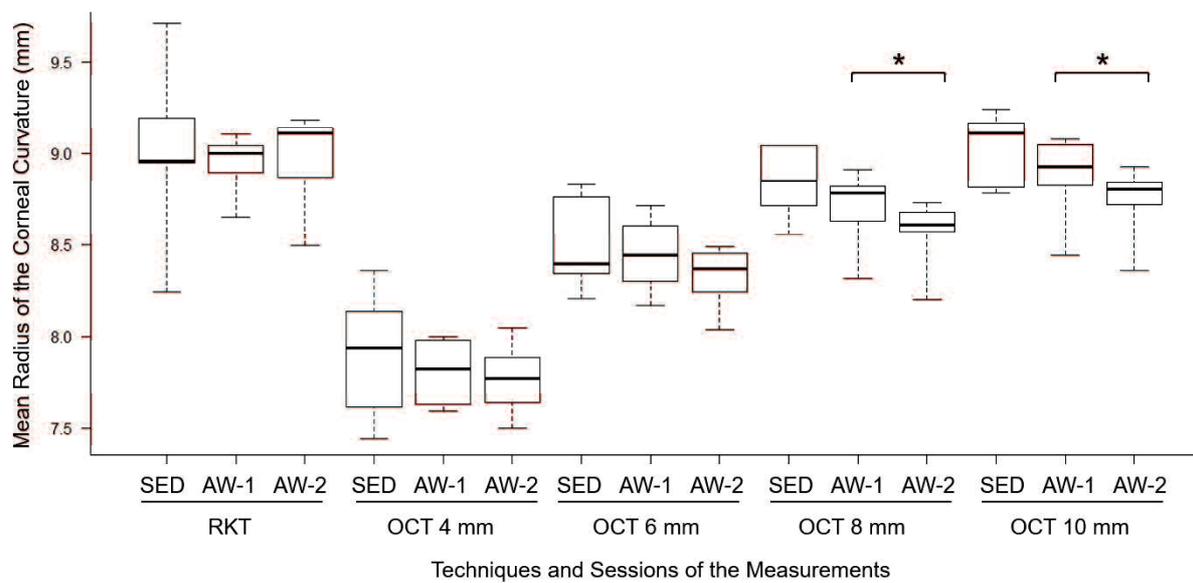
Figure 1-2. Box-and-whisker plots of the mean radius of the corneal curvature measured at different central corneal diameters using an automated handheld refractor keratometer (RKT) and a handheld anterior-segment optical coherence tomography (OCT) (n=6 dogs). The measurements were segregated by the measuring sessions, where SED represents those obtained under sedation, AW−1 represents those obtained awake on the same day as SED, and AW−2 represents those obtained awake on a different day from SED and AW−1. The median values are indicated by the horizontal line within the boxes. The first and third quartiles are represented by the lower and upper limits of the boxes. The minimum and the maximum values are shown as the lower and upper whiskers, respectively. * $P<0.05$.
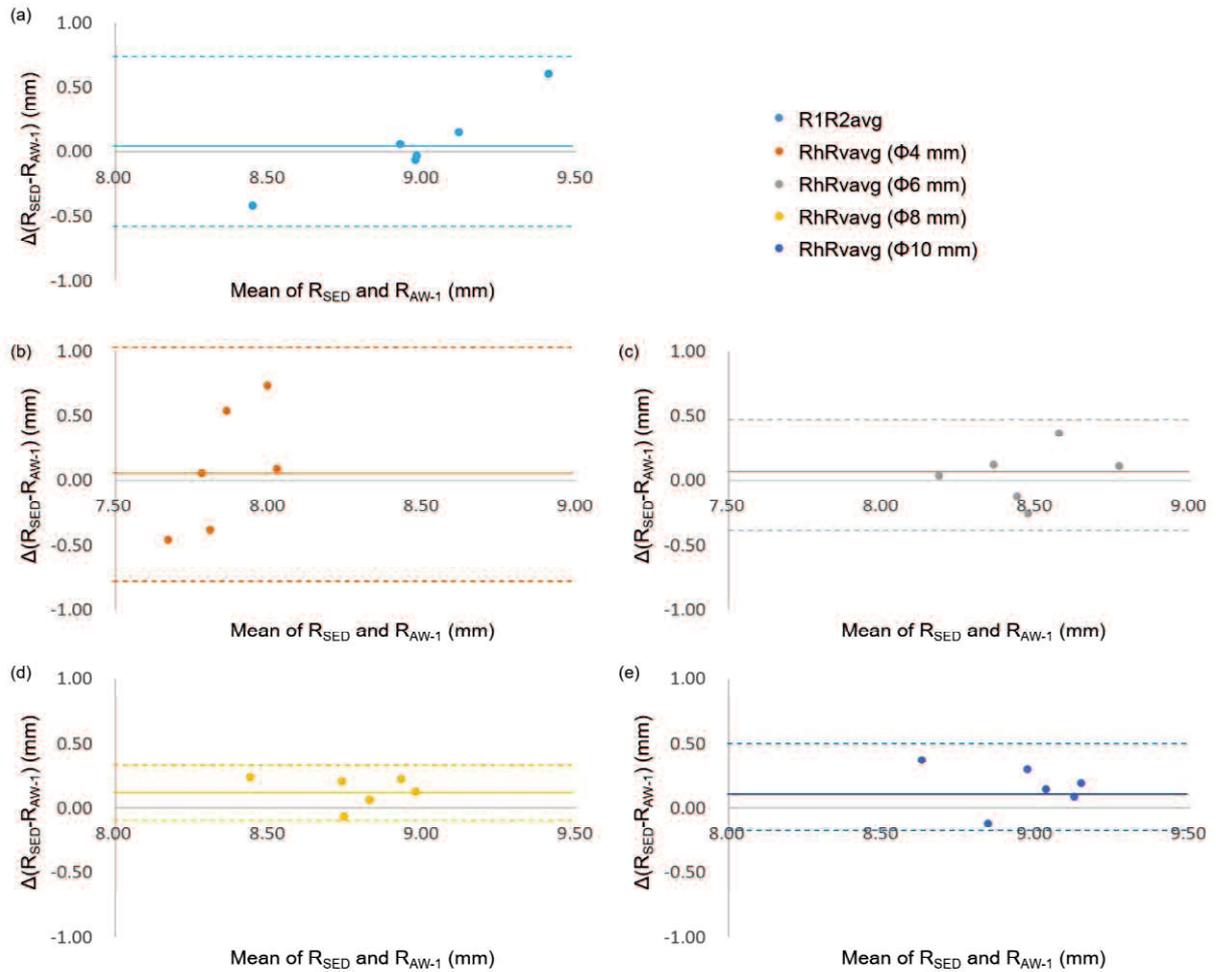
Figure 1-3. Bland-Altman plots comparing the mean radius of the corneal curvature measured under sedation (R_{SED}) and awake (R_{AW-1}) on the same day using (a) an automated handheld refractor keratometer (RKT) and (b–e) a handheld anterior-segment optical coherence tomography (OCT) (n=6 dogs). Solid lines indicate the mean of the differences. Dashed lines indicate the 95% limits of agreement as calculated by mean±1.96SD. R1R2avg=mean radius of the corneal curvature measured by RKT; RhRvavg=mean radius of the corneal curvature measured by OCT; Φ=the central corneal diameter at which the measurements were obtained by OCT.
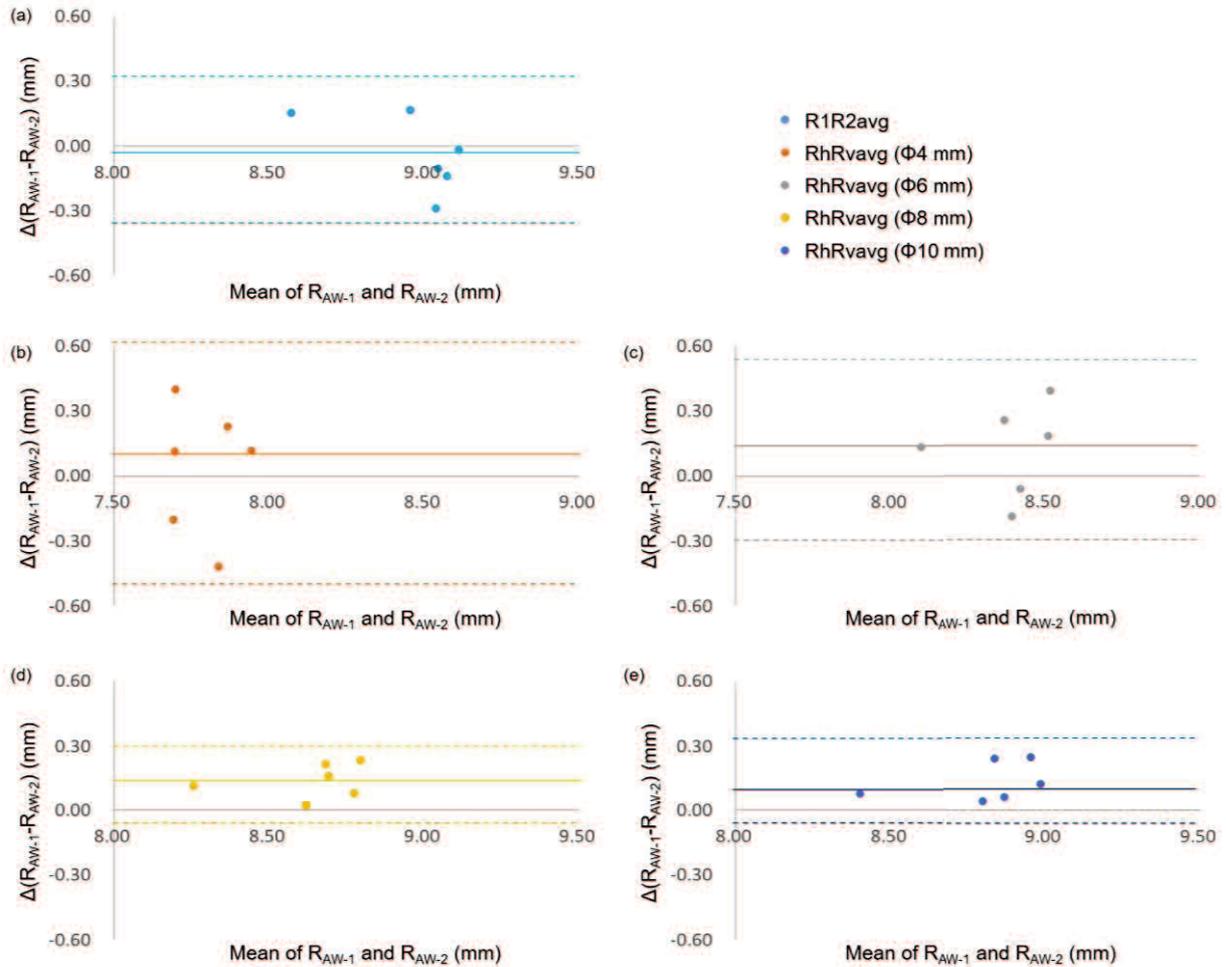
Figure 1-4. Bland-Altman plots comparing the mean radius of the corneal curvature measured awake on two different days (R_{AW-1} and R_{AW-2}) using (a) an automated handheld refractor keratometer (RKT) and (b–e) a handheld anterior-segment optical coherence tomography (OCT) (n=6 dogs). Solid lines indicate the mean of the differences. Dashed lines indicate the 95% limits of agreement as calculated by mean±1.96SD. R1R2avg=mean radius of the corneal curvature measured by RKT; RhRvavg=mean radius of the corneal curvature measured by OCT; Φ=the central corneal diameter at which the measurements were obtained by OCT.

CHAPTER 2

Comparison of keratometry using an automated handheld keratometer, optical coherence tomography, and a B-mode ultrasonography in healthy beagles

2.1 Abstract

The corneal curvature radii of seven beagles were measured using an automated handheld RKT, a handheld anterior-segment OCT, and a B-mode US. The OCT and US values were compared to those of the RKT to evaluate inter-device interchangeability. The measurements were obtained at varying central corneal diameters in 2–mm increments: RKT (4 mm), OCT (4–10 mm), and US (4–14 mm). The OCT and US values increased with increasing diameter. The RKT value was significantly larger than the OCT and US values at diameters <10 mm. The difference was the smallest when compared to OCT at 10 mm, followed by US at 12 mm. These considerable inter-device variations require cautious interpretation of the results when different devices are used.

2.2 Introduction

Keratometry, the measurement of the anterior corneal curvature, plays an important role in various clinical settings. It is routinely performed in human ophthalmology and the results are referenced when making individually tailored clinical decisions. For instance, keratometry is used to determine the appropriate base curve of a contact lens for the cornea of a patient [3–6]. It also aids in

the diagnosis of corneal diseases such as keratoconus and planning for and monitoring the outcomes of refractive surgeries [3–6]. Some of these clinical applications, especially fitting of a therapeutic contact lens, have also become increasingly popular in animals [7–18]. Consequently, it is expected that an importance of keratometry in animals become more emphasized in the field of veterinary ophthalmology.

In human ophthalmology, manual keratometry has long been considered the gold standard technique for the examination of the anterior corneal curvature [51–54]. Other techniques that provide keratometry readings include automated keratometry, slit-scanning topography, Scheimpflug topography, and OCT. The agreement of the measurements obtained using these different techniques has been evaluated extensively [51–58]. Moreover, varying degrees of inter-device interchangeability have been reported, and clinical significance has been found in some cases [51–53]. Thus, caution is advised regarding the interchangeable use of devices for patient monitoring.

In contrast, few veterinary studies have evaluated the interchangeability of keratometry techniques. Several different techniques have been used independently to evaluate keratometry in animals, some of which include manual and automated keratometry in dogs [22–24, 30] and cats [25–26, 59] and ultrasonography in horses [2, 21]. The use of OCT has been described in multiple studies on pachymetry in dogs and other species [36–38, 40–44], but not in any studies on keratometry in animals. Each of these techniques uses different measuring principles and has different advantages and disadvantages in terms of speed, reliability, and reproducibility of measurement, ease of device handling, and device availability. Thus, the present study focused on these three techniques,

namely an automated keratometer, OCT, and US. Evaluating the inter-device agreement of keratometry in dogs will help not only interpreting the measurements more accurately but also choosing more desirable technique when considering their applications in clinical settings and optometric researches.

In chapter 1, applicability of an automated handheld RKT and anterior-segment OCT in keratometry in awake dogs was successfully demonstrated using laboratory beagles. At the same time, it revealed that the keratometric values obtained by these instruments were somewhat different from each other and depending on measuring diameters. Therefore, this study aimed to measure the radii of the corneal curvature of healthy dog eyes at varying central corneal diameters using three different techniques: an automated handheld RKT, anterior-segment OCT, and B-mode US. The study also aimed to evaluate interchangeability of these devices in canine keratometry by comparing the measurements obtained by OCT and US to those obtained by the RKT.

2.3   Materials and Methods

Animals

This study included seven clinically normal adult beagles of varying ages and sexes. Thorough physical and ophthalmic examinations were conducted before their study enrolment, and normal results were found. The dogs were from the research population of the Faculty of Agriculture at Tottori University. All aspects of the study were approved by the Animal Research Committee of Tottori University (permission No.: h29-T041).

Instruments and Procedures

The radii of the anterior corneal curvature of the eye were determined using three different techniques: automated handheld RKT, handheld anterior-segment OCT, and B-mode US. The measurements with RKT, OCT, and US were made serially on both eyes in each dog. The order of measurements was determined randomly, but US was always performed last as ultrasound gel may influence RKT and OCT measurements due to the alteration of corneal reflectivity. All measurements were taken by a single examiner. The dogs were positioned in sternal recumbency and their head was manually held upright during all measurements. All dogs tolerated the procedures well without the use of sedation or general anaesthesia.

HandyRef-K (Nidek, Gamagoori, Japan) was used for RKT measurements. Keratometry examination was performed as described in chapter 1. Briefly, the device measures the anterior corneal curvature of the central 3.0–4.0 mm diameter at two axes that cross at right angles to each other. The device automatically records the radii of the flattest and the steepest corneal meridians as well as the mean of the two meridians when each measurement is completed. At least three measurements were obtained consecutively from each eye, and the average of these measurements was used for the statistical analyses.

The OCT measurements were made using a handheld swept-source anterior-segment OCT system (IVS-2000, Santec, Komaki, Japan), following the technique described in chapter 1. In short, the cornea was scanned in vertical and horizontal planes, and two-dimensional corneal images and associated per-pixel luminance data were extracted from the system. Using these data, the radii of the

corneal curvature were calculated manually at varying distances from the corneal apex, starting at 2 mm and in 1–mm increments toward the peripheral cornea. The farthest point that could be measured consistently on all images was at 5 mm. Hence, the measurements were taken at four different central corneal diameters (4, 6, 8, and 10 mm). The calculations were performed using the technique described in chapter 1, which was a method modified from that described previously [2]. The calculations were repeated at least twice for each given central corneal diameter on each plane. The values from the two planes were then averaged to determine the mean radius of the corneal curvature of a given corneal diameter.

A B-scan US unit (HI VISION Preirus, Hitachi, Chiyoda, Japan) was used to obtain trans-corneal images of the eyes. All images were obtained using a linear 13 MHz probe. Topical 0.4% oxybuprocaine solution (Benoxil, Santen, Osaka, Japan) was administered to the eye immediately prior to the examination. The probe covered with a copious amount of ultrasound gel was oriented vertically, then horizontally, on the surface of the central cornea (Figure 2-1a). An image that captured the axial length of the eye and showed minimal distortion of the cornea was recorded in each plane. The data were extracted from the system as jpg files (Figure 2-1b).

From these images, the radii of the corneal curvature were calculated manually at varying distances from the corneal apex. Starting at 2 mm from the corneal apex as in the case of OCT, the measurements were taken at six different central corneal diameters (4, 6, 8, 10, 12, and 14 mm) (Figure 2-1c). The measurements were obtained directly from the image using an Image J 1.51k (National Institutes of Health, Bethesda, MD, US) by applying the same principle used in OCT

(Figure 2-1d). At least two measurements were taken for each central corneal diameter on each plane. The average of the measurements taken from the two planes was then recorded as the mean radius of the corneal curvature of a given corneal diameter.

Statistical Analyses

A free software R version 3.4.1 (The R Foundation, Vienna, Austria) was used to analyse the data recorded above statistically. The measurements of the right and left eyes were compared using Wilcoxon signed-rank tests. Since statistically significant difference was not noted between these measurements, the mean value for each animal, based on the measurements from pairs of right and left eyes, was used in the subsequent analyses. Wilcoxon signed-rank tests were used to evaluate the differences between the measurements obtained by RKT and those obtained by OCT and US. Bland-Altman analyses were performed and the 95% LoA were calculated as the mean±1.96SD of the difference to evaluate the inter-device agreements. The data were reported as medians and range (minimum–maximum) where applicable. Statistical significance was set at $P<0.05$ in all tests.

2.4   Results

The dogs used in this study included three males and four females. Their median age and bodyweight were 6 years (1–11) and 9.0 kg (7.2–10.1), respectively. The measurements of the right and left eyes were not statistically different in all techniques (P=0.15–1.0). The median differences between the right and left eyes were 0.07 mm (0.03–0.20) with RKT, 0.05–0.09 mm (0.00–0.13) with OCT, and 0.23–0.68 mm (0.02–2.11) with US, respectively. The measurements of seven beagles

obtained with the three different techniques are shown in Figure 2-2. The median value of the mean

radius of the corneal curvature by RKT was 9.00 mm (8.45–9.11). For both OCT and US, the mean

radius of the corneal curvature increased in all dogs as the measured diameter of the central cornea

increased. The OCT measurements increased from 7.75 mm (7.24–8.00) at 4 mm diameter to 8.90

mm (8.25–9.08) at 10 mm diameter. The US measurements increased from 4.91 mm (4.48–5.62) at 4

mm to 7.86 mm (7.45–9.45) at 10 mm and further increased to 9.51 mm (9.06–10.79) at 14 mm. The

variability of the measurements among the dogs was the largest for US, followed by OCT and RKT in

decreasing order.

The median inter-device differences between the RKT and the OCT ($\Delta(R_{RKT}\text{-}R_{OCT})$) and

between the RKT and the US measurements ($\Delta(R_{RKT}\text{-}R_{US})$) are shown in Table 2-1, together with

P-values determined by Wilcoxon signed-rank tests and 95% LoA according to Bland-Altman

analyses. The OCT provided the best approximation to the RKT when the measurement was obtained

at 10 mm diameter, though the difference was statistically significant (0.11 mm, P=0.04). The mean

radius of the corneal curvature measured by US at 12 mm diameter (8.88 mm [8.65–10.23]) was also

close to the RKT reading. This was the only measurement that did not differ significantly from the

RKT reading (0.16 mm, P=0.97). All of the other measurements obtained by OCT and US were either

significantly smaller or larger than the RKT reading (P<0.01). The difference from the RKT reading

increased as the measured diameter deviated from 10–12 mm, with the absolute median differences

ranging from 0.23 to 4.06 mm.

2.5 Discussion

The results of this study revealed considerable inter-device variations in the mean radius of the anterior corneal curvature of dogs evaluated in this study. The findings also revealed that the mean radius of the corneal curvature varied greatly depending on the central corneal diameters at which the measurements were obtained. Multiple studies involving humans have reported variable inter-device agreement [51–58] and changes in the corneal curvature depending on the distance from the corneal apex [60–62]. However, few studies have investigated these aspects in the canine cornea. The present results have important implications in understanding and interpreting canine keratometry measures obtained using different techniques.

The present study mainly focused on comparing OCT and US measurements to RKT readings as keratometer is considered the gold standard technique for the measurement of the anterior corneal curvature of normal eyes in humans [51–54]. In the present study, the RKT reading was significantly larger than most of the measurements obtained by OCT and US. This is inconsistent with previously reported trends comparing keratometer readings and OCT measurements taken at around 5–6 mm diameter in humans [55, 63]. Several factors could be associated with this inconsistency, which include differences in measuring techniques and refractive indexes adopted by different devices used in each study. These factors could also have contributed to the inter-device differences observed in the present study. Most studies involving humans use OCT systems which autogenerate the measurements. On the other hand, the OCT and US measurements were obtained manually in this study. Thus, errors associated with subjective decisions cannot be eliminated from the results,

particularly for those measured at smaller diameters. Moreover, corneal contact during image acquisition by US and the lower resolution of the US images compared to that of the OCT images may have affected the results by negatively affecting the accuracy of the measurements. It is important to be aware that RKT readings are not necessarily interchangeable with other devices; thus, the results must be interpreted with caution when various techniques are used for keratometry in dogs.

The mean radius of the corneal curvature of beagle dogs increased as the central corneal diameter of measurement increased in both OCT and US. Although the magnitudes of the changes were much larger for US than for OCT, the trend observed between these techniques was similar. This result implies that the anterior corneal curvature of beagles is steeper centrally and becomes flatter toward the periphery, as also reported in humans [60–62]. Additionally, the deviations from the RKT reading were the smallest when the measurements were taken at 10 mm and 12 mm diameters with each device. Although the measuring diameter of the RKT indicated approximately 4 mm, the measurement may instead reflect the corneal curvature at a much larger diameter. This may be because the cornea of beagles was not spherical, thus the measurements with RKT may not be accurate. Alternatively, it may be possible that the keratometer is designed to autogenerate the estimated radius of the more peripheral cornea based on an internal calibration and algorithm in order to suffice practical needs. In general, the corneal diameter of humans is approximately 12 mm [64–65] and the diameter of rigid gas permeable contact lenses commonly prescribed for humans is around 10 mm. Thus, the peripheral corneal curvature is clinically more important than the central curvature for the selection of a parallel-fitting contact lens for normal corneas [62]. Detailed topographic studies are

needed to characterize the true corneal curvature of dogs and to validate the accuracy of the RKT readings with respect to the diameter of measurement.

Nonetheless, major advantages of an automated keratometer include the ability to obtain multiple measurements rapidly and consecutively without direct corneal contact. The use of keratometers has been described in several studies involving dogs [22, 30]. The smaller variability associated with the RKT is also a favourable feature. The variability associated with OCT was only slightly larger than that of the RKT. However, the variability associated with US was much larger than that of the RKT and OCT. Thus, the accuracy of measurements made by RKT and OCT are superior to those made by US regardless of the diameter.

Anterior-segment OCT is a relatively new, more sophisticated technique. Although its accessibility in veterinary practices remains limited, its advantages include that it can acquire higher resolution corneal images with no direct corneal contact. It can also provide detailed topographic and pachymetric information besides keratometry. The validity and repeatability of the corneal curvature measurements using an OCT system have been studied in humans [55–58, 63]. However, studies in veterinary ophthalmology have been limited to those describing normal and pathological corneal conditions [45, 66] and evaluating its applicability for corneal pachymetry [36–44]. The present study, together with that described in chapter 1, is the first to evaluate the applicability of OCT for keratometry in dogs using laboratory beagles.

B-mode US is primarily used for diagnostic purposes in clinical settings and for research studies on corneal pachymetry [38, 40] and ocular biometry [67-70]. Several studies have described

its application to keratometry in horses [2, 21]. However, US is rarely used for keratometry in other species, including dogs and humans. One of the major advantages of US is the wide availability of the device in most veterinary practices. However, the variability observed in this study raises concerns regarding the accuracy and reliability of measurements obtained by US. Additionally, this technique requires corneal contact with the ultrasound probe to acquire the images. This could distort the cornea during image acquisition, potentially affecting the measurements.

This study has several limitations, including the small sample size consisting only of a single breed of dogs. A single examiner conducted all the examinations to obtain the measurements. This allowed sufficient time to acclimatise the dogs to undergo examination without sedation and to train the examiner to smoothly and consistently handle the devices and use the software. However, further studies are needed to validate the applicability of these results in other dog breeds and to evaluate the inter-examiner repeatability. Additional studies involving increased numbers of dogs with various signalment and multiple examiners are also needed.

In conclusion, considerable inter-device variations were noted when the mean radius of the corneal curvature of beagle dogs was measured using three different techniques. The difference from the RKT reading was smaller for OCT than for US and decreased as the measuring diameter approached 10–12 mm. Among the techniques evaluated in this study, the RKT was the fastest and easiest technique for obtaining multiple measurements at a pre-determined diameter, with minimal stress on the dogs during examination. OCT appeared to have a level of reliability similar to that of the RKT but was more technically demanding and expensive. US was the most accessible and a more

familiar device to practicing veterinarians; however, the measurements showed larger deviations from

the RKT readings and much greater variability compared to RKT and OCT. One should understand

the features of each technique and choose the measurement technique accordingly. These results

suggested that the measurements obtained by the different techniques and at different diameters

should be interpreted with caution as the measurements are not necessarily interchangeable.

2.6　Tables and Figures

Table 2-1. Summary of inter-device differences in the mean radius of the corneal curvature measurements compared to the keratometer reading (n=7 dogs). P-values were determined by Wilcoxon signed-rank tests. The 95% limit of agreement (LoA) was calculated as the mean±1.96SD of the difference according to Bland-Altman analyses.

Pair of Devices	Median Difference (Minimum, Maximum)		P	95%LoA	
				Lower	Upper
$\Delta(R_{RKT}-R_{OCT4})$	1.22	(0.75, 1.41)	<0.01	0.72	1.58
$\Delta(R_{RKT}-R_{OCT6})$	0.50	(0.39, 0.74)	<0.01	0.27	0.78
$\Delta(R_{RKT}-R_{OCT8})$	0.23	(0.08, 0.41)	<0.01	0.04	0.48
$\Delta(R_{RKT}-R_{OCT10})$	0.11	(-0.15, 0.22)	0.04	-0.17	0.36
$\Delta(R_{RKT}-R_{US4})$	4.06	(3.03, 4.62)	<0.01	2.81	5.02
$\Delta(R_{RKT}-R_{US6})$	3.29	(1.48, 3.48)	<0.01	1.42	4.44
$\Delta(R_{RKT}-R_{US8})$	1.43	(-0.61, 1.90)	<0.01	-0.61	3.02
$\Delta(R_{RKT}-R_{US10})$	1.19	(-0.80, 1.45)	<0.01	-0.76	2.51
$\Delta(R_{RKT}-R_{US12})$	0.16	(-1.58, 0.28)	0.97	-1.58	1.24
$\Delta(R_{RKT}-R_{US14})$	-0.45	(-2.14, -0.17)	<0.01	-2.16	0.71

R_{RKT}=mean radius of the corneal curvature measured by an automated handheld refractor keratometer (RKT); R_{OCT}=mean radius of the corneal curvature measured by a handheld anterior-segment optical coherence tomography (OCT); R_{US}=mean radius of the corneal curvature measured by a B-mode ultrasonography (US). The numerical figures following "OCT" and "US" indicate the central corneal diameter at which the measurement was obtained.
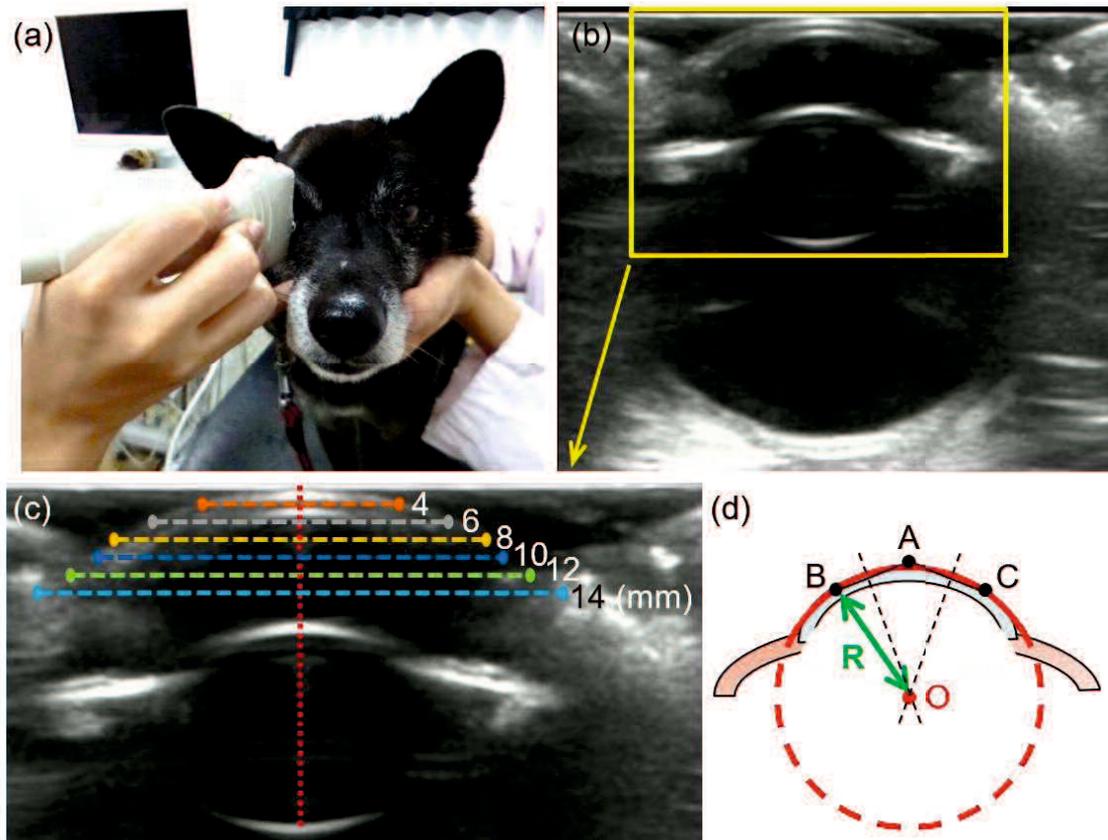
Figure 2-1. (a) Trans-corneal scan of the eye using a B-mode ultrasonography (US). (b) A representative image of an eye obtained by US. (c) The close-up of an area enclosed by a yellow rectangle on the image (b), showing anterior segment of the eye and the central corneal diameters at which the measurements were obtained by US. (d) A schematic diagram illustrating the measurement technique. Point A represents the corneal apex. Point B and C represent the points located at a given distance from the corneal apex. Dashed lines represent the perpendicular bisectors of the line AB and AC, respectively. Point O represents the point of intersection of the two bisectors, which represents the centre of the corneal curvature. Distance R represents the radius of the corneal curvature.
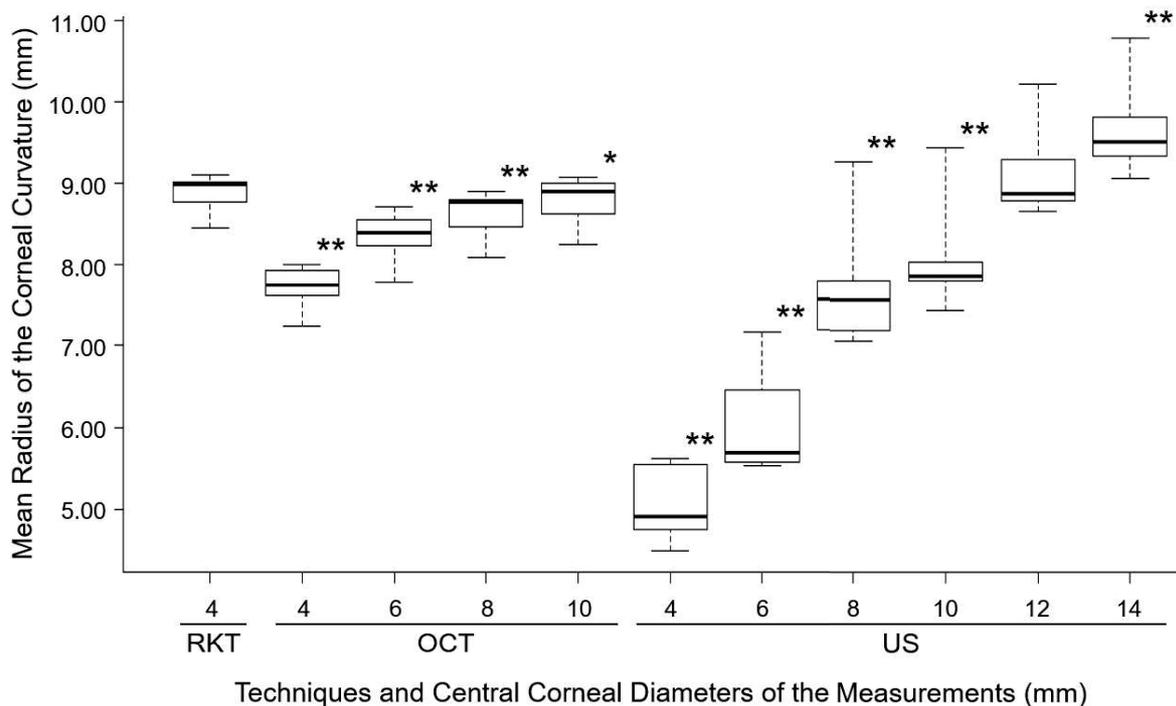
Figure 2-2. Box-and-whisker plots of the mean radius of the corneal curvature measured at different central corneal diameters using an automated handheld refractor keratometer (RKT), a handheld anterior-segment optical coherence tomography (OCT), and a B-mode ultrasonography (US) (n=7 dogs). The median values are indicated by the horizontal line within the boxes. The first and third quartiles are represented by the lower and upper limits of the boxes. The minimum and the maximum values are shown as the lower and upper whiskers, respectively. * P<0.05 and ** P<0.01 when compared with the mean radius of the corneal curvature measured with RKT.

CHAPTER 3

Evaluation of corneal topography in normal beagles and mixed-breed cats using hard contact lenses and its association with keratometry using an automated handheld keratometer

3.1 Abstract

Six beagles and eight mixed-breed cats were used to evaluate corneal topography using HCLs with 8–14 mm diameters and to assess its association with keratometry obtained by RKT. The median base curve of a parallel-fitting HCL determined by fluorescein pooling patterns increased with increasing lens diameter in both dogs (8.85–9.35 mm) and cats (8.55–9.20 mm). The median keratometric value was 9.03 mm in dogs and 8.79 mm in cats, which showed better agreement with the parallel-fitting base curves of 8–10 mm diameter lenses. The results indicated that the corneal shape of the animals evaluated in this study was steeper centrally and became flatter toward periphery. The RKT reading reflected more peripheral corneal curvature. The results are clinically important when designing and fitting contact lenses for dogs and cats.

3.2 Introduction

Rigid gas-permeable contact lenses, or HCLs, are commonly used to achieve optical correction in humans. They are made of durable plastic material and maintain its shape on the corneal

surface [71]. Thus, fluorescein dye has long been used to evaluate the relationship between the HCL

and the corneal surface [72]. Differing fluorescein pooling patterns observed with slit lamp can be

used to estimate the shape of the anterior cornea, or corneal topography.

Shape of HCLs is specified with base curve and diameter. Base curve represents the radius

of curvature of the posterior surface of a lens. Diameter represents the size of a lens. Although other

parameters also need to be considered when fitting a HCL to a cornea, an initial trial lens is usually

chosen empirically based on keratometer readings [71]. Then, fitting of a HCL to the cornea is

evaluated subjectively using fluorescein dye [71, 73]. This technique utilises the fact that differing

fluorescein patterns can be seen depending on the lens-to-cornea relationship. While there are many

factors which may affect the pattern, it has been the conventional and recommended technique to

determine the final lens in humans [71]. The fit between the lens and the anterior corneal surface plays

an important role in improving not only the comfort but also the safety and efficacy of contact lens

wear. The shape of the peripheral cornea is particularly important to achieve an optimum fitting of

contact lenses.

In chapter 2, the study revealed some variations in the corneal curvature radius in beagle

dogs depending on the measuring techniques and the distance from the corneal apex at which the

measurements were obtained. The lack of comparative studies which evaluated inter-device

interchangeability and corneal topography of dogs left room for further studies to validate reliability

of the results. In humans, there are multiple studies which investigated inter-device variations in the

corneal curvature measurements [3, 51–58, 74–75]. It is also widely recognised that the shape of the

cornea changes, or flattens, with increasing corneal diameters [60–62]. It would be worth investigating whether such variations are also present in dogs and cats or the findings in chapter 2 were associated with measurement errors.

There has been an increasing interest in the use of therapeutic contact lenses in treatment of various corneal diseases in dogs and cats [7–15]. Understanding the corneal contour of dogs and cats in more details would help improving therapeutic interventions provided by veterinary practitioners as well as contact lens designs developed for use in dogs and cats. Therefore, the present study aimed to evaluate the shape of the anterior corneal curvature of dogs and cats at varying distances from the corneal apex using HCLs and fluorescein dye. The study also aimed to evaluate association between the best-fit base curve of HCLs determined by fluorescein pooling patterns and keratometer readings.

3.3   Materials and Methods

Animals

The study used six beagles and eight mixed-breed cats of varying ages and sexes. The dogs were from the research population of the Faculty of Agriculture, and the cats from that of the Faculty of Medicine, at Tottori University. All animals were identified as clinically normal following thorough physical and ophthalmic examinations. All aspects of the study were approved by the Animal Research Committee of Tottori University (permission No.: h29-T041 and h30-T045).

Procedures

Keratometry was performed to determine mean radius of the anterior corneal curvature of

the eye using an automated handheld RKT, HandyRef-K (Nidek, Gamagoori, Japan). At least three

measurements were obtained from both right and left eyes in each animal, and the average of these

measurements was calculated. Details of the measuring technique and setting of the device were as

described in chapter 1.

HCLs with varying specifications were fitted to the cornea and the best-fit base curve of a

lens with a particular diameter was determined. Base curve of the first trial lens was chosen

empirically based on the RKT reading. A total of 33 lenses were specifically designed for use in this

study (Seed, Hongo, Japan). Specifications of the HCLs included three different diameters (8, 10, and

14 mm) and 11 different base curves (8.0–10.0 mm in 0.2–mm increments) for each of the three

diameters. The lenses were fitted to the cornea of one eye in each animal to minimise stress associated

with the handling. The eye was selected randomly.

Prior to application of a lens, a drop of 0.4% oxybuprocaine ophthalmic solution (Benoxil,

Santen, Japan) was administered to the eye. A drop of 10% fluorescein isothiocyanate-dextran

solution (FITC-dextran, Sigma-Aldrich, St. Louis, MO, US) was placed on the posterior surface of the

lens, and the lens was gently applied to the cornea. Fitting of a lens was evaluated using slit lamp with

a blue light. Lens-to-cornea relationship was determined based on an observation of fluorescein

pooling pattern between the lens and the cornea and classified as either steep, parallel, or flat

subjectively (Figure 3-1). Fitting was classified as steep when most of the dye pooled at the centre of

the lens, or at the corneal apex, or when air bubble was trapped between the lens and the cornea. This

occurs when the base curve of a HCL is smaller than true radius of the corneal curvature. Fitting was

classified as flat when the dye pooled at the periphery of the lens. This occurs when the base curve of a HCL is larger than true radius of the corneal curvature. Fitting was classified as parallel when the dye was distributed uniformly between the lens and the cornea. This occurs when the base curve of a HCL is similar to true radius of the corneal curvature.

The procedure was repeated one after another by replacing the lens with one step larger or smaller base curve lenses at a time until steep and flat fitting patterns were observed for each diameter. The base curve of a parallel-fitting HCL was considered as the best-fit base curve at the particular diameter. When the steep- and flat-fitting fluorescein patterns were noted consecutively with the two adjacent base curves, and the parallel-fitting pattern was not observed in between, the midpoint value of the steep- and flat-fitting base curves was taken as the best-fit base curve.

Throughout the examinations, animals were positioned in sternal recumbency and the head was held upright manually. All of the procedures were tolerated well by all animals without using sedation or general anaesthesia. All measurements with the RKT and HCL fitting evaluations were performed by a single examiner.

Statistical analyses

A free software R version 3.4.1 (The R Foundation, Vienna, Austria) was used for statistical analyses. The measurements of the right and left eyes obtained with RKT were compared using Wilcoxon signed-rank tests. Mean radius of the corneal curvature measured by RKT (R_{RKT}) and the best-fit base curve of a HCL (R_{HCL}) with three different diameters were compared using Wilcoxon signed-rank tests. For the purpose of this study, it was considered that the best-fit base curve of a HCL

with a particular diameter closely represents the true radius of the anterior corneal curvature at the

particular diameter. Statistical significance was set at P<0.05 in all tests.

3.4 Results

The dogs used in this study included three males and three females. Their age and

bodyweight ranged from 1 to 12 years (median: 5) and from 7.2 to 9.3 kg (median: 8.9), respectively.

R_{RKT} of the dogs ranged from 8.53 to 9.11 mm (median: 9.03). Statistically significant differences

were not noted between the measurements from pairs of right and left eyes (P=1.0). R_{HCL} with the

diameter of 8, 10, and 14 mm ranged from 8.50 to 9.00 mm (median: 8.85), from 8.60 to 9.20 mm

(median: 9.05), and from 9.10 to 9.60 mm (median: 9.35), respectively (Table 3-1). The difference

between R_{RKT} and R_{HCL} ($\Delta(R_{RKT}-R_{HCL})$) with three different diameters ranged from -0.09 to 0.26 mm

(median: 0.07, P=0.22), from -0.29 to 0.06 mm (median: -0.08, P=0.16), and from -0.69 to -0.20 mm

(median: -0.50, P=0.03), respectively (Figure 3-2a).

The cats used in this study included four males and four females. Their age and bodyweight

ranged from 0.8 to 11.2 years (median: 4.3) and from 2.5 to 4.1 kg (median: 2.9), respectively. R_{RKT} of

the cats ranged from 8.40 to 8.93 mm (median: 8.79). Statistically significant differences were not

noted between the measurements from pairs of right and left eyes (P=0.64). R_{HCL} with the diameter of

8, 10, and 14 mm ranged from 8.30 to 8.90 mm (median: 8.55), from 8.40 to 9.10 mm (median: 8.75),

and from 8.70 to 9.30 mm (median: 9.20), respectively (Table 3-1). $\Delta(R_{RKT}-R_{HCL})$ with three different

diameters ranged from -0.10 to 0.30 mm (median: 0.11, P=0.05), from -0.20 to 0.18 mm (median:

-0.05, P=0.58), and from -0.60 to -0.21 mm (median: -0.41, P<0.01), respectively (Figure 3-2b).

Figure 3-3 shows typical fluorescein pooling patterns observed with slit lamp in a dog and a cat, respectively. In all animals evaluated in this study, R_{HCL} increased as the diameter of the lens increased. While R_{RKT} generally showed good agreement with R_{HCL} of 8 and 10 mm diameter lenses in both dogs and cats, it was much smaller than that of 14 mm diameter lens.

3.5 Discussion

The present study used HCLs with varying specifications and fluorescein dye to visually assess the shape of the anterior cornea in beagle dogs and mixed-breed cats. An increasing R_{HCL} with the increasing lens diameter in both species indicates that the anterior corneal curvature of dogs and cats evaluated in this study is steeper centrally and flatter peripherally. In other words, the mean radius of the corneal curvature is smaller centrally and larger peripherally. The present study only involved small numbers of dogs and cats. The breeds and genetic variations of the animals evaluated were also limited because they were sourced from research populations. Thus, the results of this study may not be directly applicable to general canine and feline populations. However, to the authors' knowledge, this is the first study which evaluated the anterior corneal curvature of healthy dogs and cats at various distances from the corneal apex using HCLs and fluorescein dye.

The trend of increasing corneal curvature radius from the centre to periphery was consistent with that widely recognised in humans [60–62]. The finding was also in accordance with the trend noted in the study described in chapter 2 using an OCT and B-mode US. It is interesting to note that

the rate of changes found in this study was much greater than that reported in humans. The present study found that R_{HCL} increased by 0.2 mm when the lens diameter increased from 8 to 10 mm, and by further 0.3 mm when it increased from 10 to 14 mm. In contrast, the change reported in human cornea was by an approximately 0.05 mm increase with increasing corneal diameters from 6 to 10 mm [61]. While the central cornea is the most important area for vision, the peripheral cornea also plays some roles in off-axis aberrations and vision [61]. The marked changes in the curvature from the central to the peripheral cornea in dogs and cats, comparing with human cornea, may be associated with their evolutional adaptation as predator species. Besides, the peripheral corneal contour is important for contact lens fitting. Hence the result has a clinically important implication when therapeutic contact lenses are designed and prescribed for dogs and cats.

In the present study, it was considered that R_{HCL} with a particular diameter closely represents the true radius of the anterior corneal curvature at the particular central corneal diameter. This is based on the fact that a HCL does not change its shape following its application to the cornea, thus a parallel-fitting HCL aligns the shape of the cornea more closely than steep- or flat-fitting HCLs [71, 73]. Comparisons between R_{HCL} and R_{RKT} revealed that R_{RKT} was in the best agreement with R_{HCL} with 8–10 mm diameters in both dogs and cats. The similar result was also noted in the study described in chapter 2, where the RKT reading was compared with the OCT values obtained at varying central corneal diameters between 4 and 10 mm using beagle dogs. The differences between the two techniques were the smallest when the RKT reading was compared with the OCT value measured at 10 mm diameter and increased with decreasing diameters of the measurements. These

results together suggested that the RKT reading is likely to represent the true corneal curvature radius at approximately 8–10 mm diameters rather than 4 mm as indicated by the manufacturer at least in the animals evaluated in this study.

Assessment of the fluorescein patterns in HCL fitting possesses some subjectivity, which is an inherent disadvantage of the technique. The present study did not evaluated inter-examiner variations as all examinations were conducted by a single examiner. This left room for further studies to validate repeatability of the results when multiple examiners were involved. Nonetheless, this is a recommended technique to assess lens-to-cornea fit when a HCL is prescribed in humans [71, 73]. This does not exclude the cases where the corneal curvature is predetermined via keratometry or more sophisticated corneal analysers such as topographic or tomographic devices [73]. Classification of fluorescein patterns into steep, parallel, or flat is relatively straightforward and a guideline can easily be found in literatures [73]. Fluorescein pooling can be noted by human eyes when it has a thickness of at least 20 μm [73]. Therefore, the technique is clinically useful to determine the area that the posterior surface of the lens is in contact with the anterior surface of the cornea, where it appears dark even with the fluorescein dye.

In summary, HCLs with varying specifications were useful to demonstrate the corneal topography of dogs and cats based on fluorescein pooling patterns between the lens and the cornea. This technique demonstrated that the corneas of beagle dogs and mixed-breed cats evaluated in this study flattened toward periphery as recognised in humans, but at much greater rate. Additionally, the study found that the mean radius of the corneal curvature obtained by the automated handheld RKT

was the most representative of the true curvature at the central corneal diameter of 8−10 mm. Although further studies would be warranted to validate applicability of the results to general dog and cat populations due to limited sample size and breed variations, the present study has important implications both clinically and scientifically when designing and fitting a therapeutic contact lens to the corneas of these species and when interpreting their vision.

3.6 Tables and Figures

Table 3-1. Summary of signalment, bodyweight, the mean radius of the corneal curvature measured by an automated handheld refractor keratometer (R_{RKT}), and the base curve of parallel-fitting hard contact lenses (R_{HCL}) determined based on fluorescein pooling pattern in each animal evaluated in this study. The numerical figures following "HCL" indicate the diameter of a lens.

Animal	Sex	Age (years)	Bodyweight (kg)	R_{RKT} (mm)	R_{HCL8} (mm)	R_{HCL10} (mm)	R_{HCL14} (mm)
Dogs							
1	Male	1	8.7	8.53	8.50	8.60	9.10
2	Female	4	8.8	8.71	8.80	9.00	9.40
3	Male	6	7.2	9.00	9.00	9.20	9.50
4	Female	12	9.0	9.06	8.80	9.00	9.30
5	Male	1	9.3	9.11	8.90	9.10	9.30
6	Female	11	9.2	9.11	9.00	9.20	9.60
Cats							
1	Female	6.4	2.6	8.40	8.50	8.60	9.00
2	Female	0.8	2.6	8.49	8.30	8.40	8.70
3	Male	10.3	3.8	8.72	8.70	8.80	9.20
4	Male	2.3	3.5	8.78	8.50	8.60	9.20
5	Female	2.3	2.5	8.80	8.50	8.70	9.00
6	Male	1.6	3.1	8.80	8.60	8.80	9.20
7	Male	7.3	4.1	8.81	8.80	8.90	9.30
8	Female	11.2	2.7	8.93	8.90	9.10	9.30
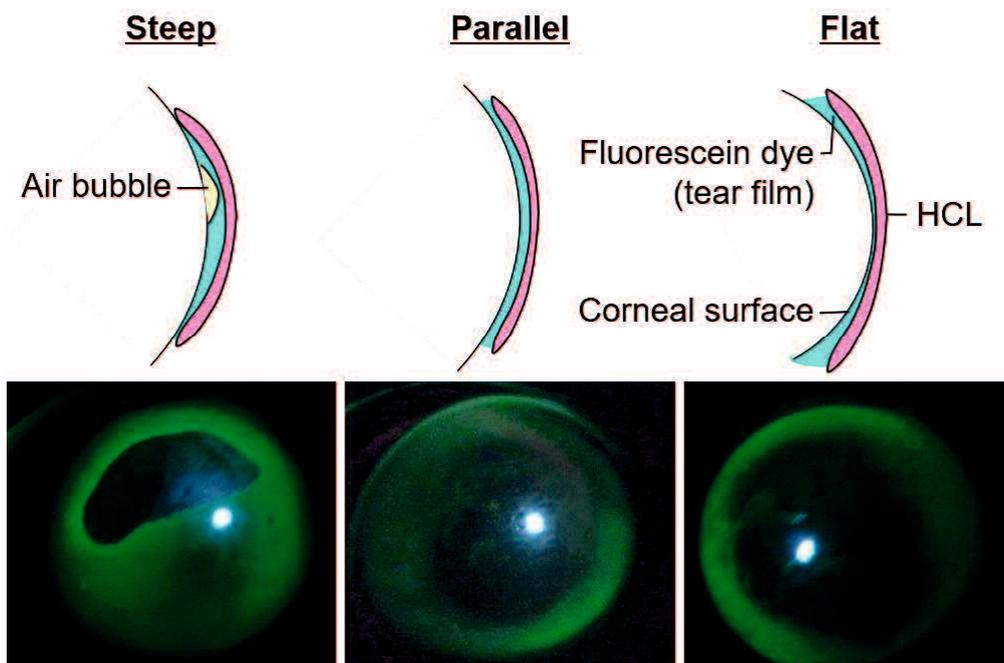
Figure 3-1. Schematic diagrams (top) and typical slit lamp images observed with a blue light (bottom) illustrating the lens-to-cornea relationships determined based on fluorescein pooling pattern. Fitting was classified as steep when most of the dye pooled at the centre of the lens, or at the corneal apex, or when air bubble was trapped between the lens and the cornea. It was classified as flat when the dye pooled at the periphery of the lens. It was classified as parallel when the dye was distributed uniformly between the lens and the cornea. HCL=hard contact lens.

(a)

(b)
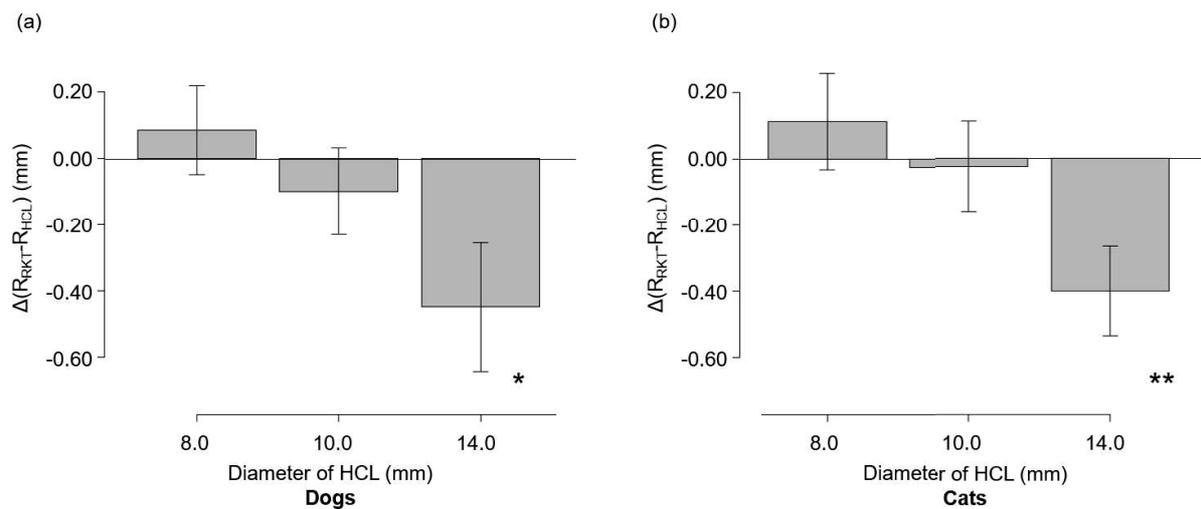
Figure 3-2. Bar graphs show differences between the mean radius of the corneal curvature measured by an automated handheld refractor keratometer (R_{RKT}) and the base curve of a parallel-fitting hard contact lens (R_{HCL}) determined by fluorescein pooling pattern ($\Delta(R_{RKT}-R_{HCL})$) in (a) dogs and (b) cats. Bars represent standard deviations. * $P<0.05$ and ** $P<0.01$ when compared with R_{RKT} using Wilcoxon signed-rank tests.
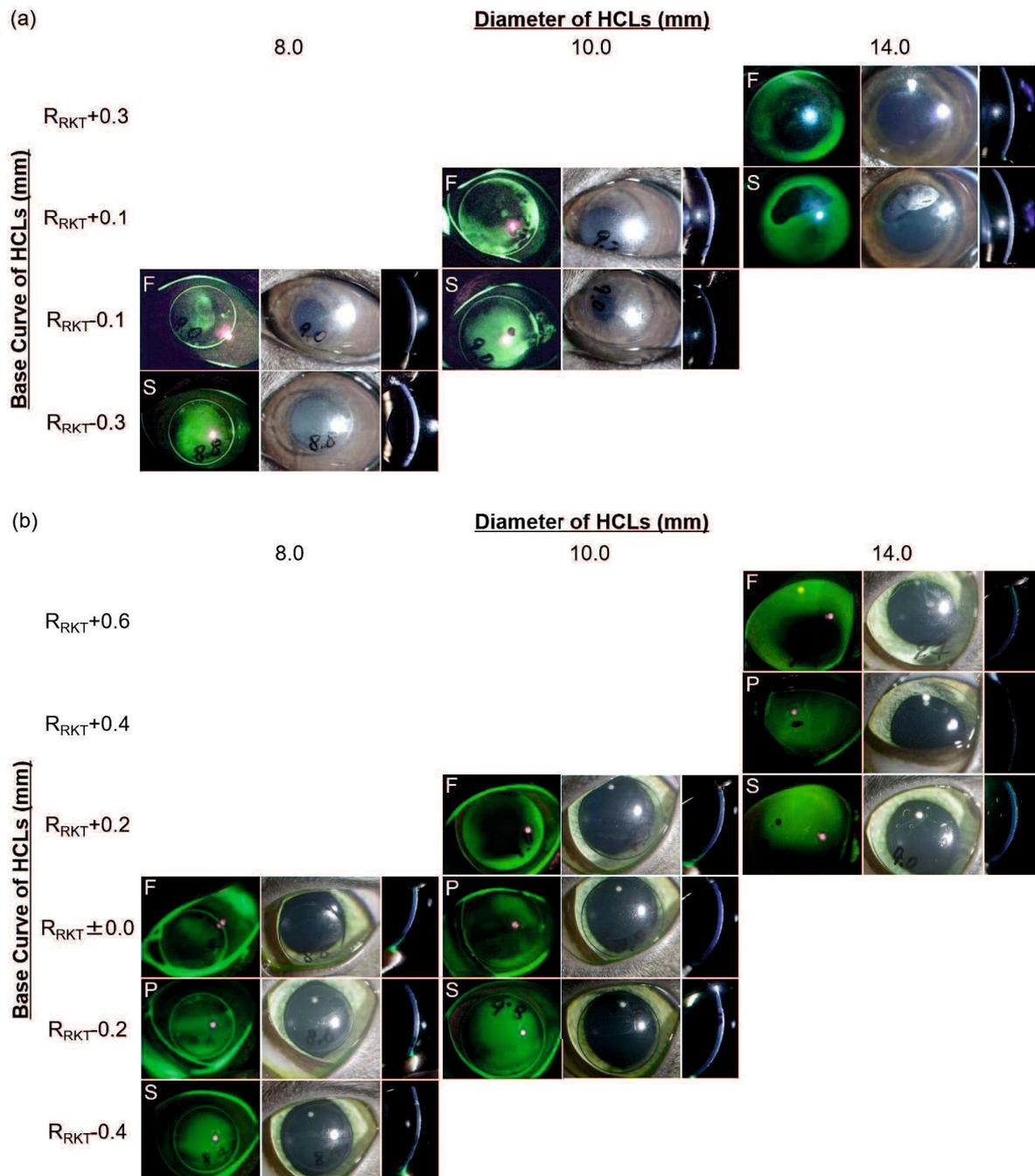
Figure 3-3. Images show typical fluorescein pooling patterns observed with slit lamp in (a) a dog and (b) a cat following application of hard contact lenses (HCLs) with varying specifications. "S" indicates steep-fitting HCLs, where fluorescein dye pooled centrally. "P" indicates parallel-fitting HCLs, where fluorescein dye was distributed uniformly. "F" indicates flat-fitting HCLs, where fluorescein dye pooled peripherally. "R_{RKT}" indicates mean radius of the corneal curvature measured by an automated handheld refractor keratometer.

CHAPTER 4

Characterising keratometry in different dog breeds using an automated handheld keratometer

4.1 Abstract

Keratometry was performed prospectively in 237 dogs from 16 different breeds using an automated handheld RKT. The study aimed to describe breed-specific keratometry of dogs which are popular in Japan. Inter-breed variations in R1R2avg and the degree of corneal astigmatism ($|\Delta(R1-R2)|$) were also evaluated statistically with respect to their bodyweight. R1R2avg (mean±SD) ranged from 7.54±0.30 mm in Pomeranians to 9.28±0.19 mm in Golden Retrievers. $|\Delta(R1-R2)|$ (mean±SD) ranged from 0.22±0.11 mm in Miniature Schnauzers to 0.57±0.30 mm in French Bulldogs. Considerable inter-breed variations were noted in both R1R2avg and $|\Delta(R1-R2)|$, which did not necessarily correlated with their bodyweight. These results have important implications both clinically in the management of corneal diseases and non-clinically in optometric studies in dogs.

4.2 Introduction

Keratometry is defined as the measurement of corneal curvature, which determines the power of the cornea and astigmatism [2–3]. It is an essential part of ophthalmic examinations in human ophthalmology. The values of the mean corneal curvature are referred to in various clinical

51

settings such as fitting contact lenses, determining intraocular lens power, and evaluating corneal astigmatism in association with various corneal refractive surgeries [3–6].

In dogs, fitting of a contact lens has been reported to correct aphakia [7] and to provide support to the corneal surface during treatment of various corneal diseases, such as spontaneous chronic corneal epithelial defects, superficial and stromal corneal ulcers, corneal calcareous degeneration, and corneal dystrophy [8–15]. Additionally, cataract extraction surgeries, which potentially create corneal astigmatism, have become increasingly popular over the past few decades [18]. It is expected that details of keratometry in different dog breeds provide valuable information to further optimise therapeutic interventions offered to individual patients. Such data would be especially valuable in dogs due to the large morphological variations between breeds.

Several studies have documented keratometry in dogs using manual and automated keratometers [22–24, 30]. One of the major advantages of an automated keratometer is its ability to measure corneal curvatures rapidly within a few seconds [3, 31–33]. The applicability of automated handheld keratometers in awake dogs was evaluated by Gorig *et al* [30] and in the study described in chapter 1. Both of these studies demonstrated that the measurements obtained awake and under sedation or general anaesthesia were comparable. This result was encouraging and has led to such keratometers gaining popularity in the field of veterinary ophthalmology.

Although some data have been published regarding keratometry in dogs, details of keratometry in different breeds have not yet been reported. The breeds covered in previous studies are limited, with relatively small sample sizes of miniature breeds, which are more commonly seen in

Japan [23–24, 30]. Hence, little is known about the normal values of corneal curvatures in dogs of various breeds, particularly measurements obtained when awake using an automated handheld keratometer. Therefore, the present study aimed to describe the reference values for breed-specific corneal curvature and corneal astigmatism in some dog breeds popular in Japan. Additionally, the study evaluated inter-breed and intra-breed variations in the mean corneal curvature and the degree of corneal astigmatism observed in dogs of various age and bodyweight.

4.3   Materials and Methods

Animals

Client-owned dogs of various breeds, sex and age presented to the Tottori University Veterinary Medical Centre (TUVMC) between April 2017 and December 2018 were included in the study. The dogs were first evaluated for their eligibility for enrolment in the study according to the following inclusion criteria:

1. General health conditions and characteristics: the dog was clinically stable and could tolerate manual restraint of the head for thorough ophthalmic and keratometry examinations without sedation or general anaesthesia.

2. Age: the dog was aged 10 months or older.

3. Ocular health: the dog had no ocular or periorbital diseases which could potentially affect ocular morphology or corneal conformations of both eyes at the time of examination. Such diseases included, but were not limited to, corneal diseases such as corneal ulcers and oedema;

glaucoma; and ocular, retrobulbar or periorbital neoplasia.

Dogs that met all of these criteria at the time of presentation underwent keratometry examination prospectively. All aspects of the study were approved by the Animal Clinical Research Ethics Committee of Tottori University (permission No.: H29-006). Full consent was obtained from all dog owners using printed documents before examinations.

Procedures

An automated handheld RKT, HandyRef-K (Nidek, Gamagoori, Japan), was used to perform the keratometry examinations. The measurements of both R1 and R2, as well as R1R2avg were recorded following the technique described in chapter 1. Briefly, the dogs were positioned either in sternal recumbency or sitting position on an examination table. The head of the dog was manually held upright so that the muzzle pointed forward and was parallel to the floor. The instrument was held in front of the eye so that the centre of the eye matched the centre of the reference ring image displayed on the device screen. The measurement was taken repeatedly to obtain at least three readings and up to 10 stable readings on each eye, depending on how tolerant the dog was of the examination. Keratometry was performed on both eyes one after another in a single session. All measurements were performed by a single examiner to eliminate inter-examiner variability. The measurements were expressed in millimetres, and were recorded to the nearest 0.01 mm.

Statistical Analyses

To facilitate statistical analyses, the data were first evaluated for their suitability for inclusion in the statistical analyses according to the following criteria:

4. Reliable measurement: both the right and left eyes were measured successfully, and the difference in the R1R2avg between the right and left eyes was less than 4.5%.

5. Sample size sufficient for statistical examination: data from more than five individuals per breed were available when the dogs were classified by breeds.

The data which did not satisfy either or both of these criteria were excluded from statistical analyses. Criterion 4 was set to assure the reliability of measurements by comparing between the eyes of the same individual. It was assumed that the normal corneas of a healthy dog would yield similar keratometry readings between the right and left eyes, as reported previously [23–24]. A difference greater than 4.5% between the eyes of an individual dog was considered a measurement error attributable to the dog, such as failure of visual fixation and existence of non-diagnosed or subclinical ocular pathologies. A threshold of 4.5% was set based on the results of a preliminary study which evaluated intra-examiner variability using extracted porcine globes. Criterion 5 was set to allow statistical analyses of the data classified by breeds.

Statistical analyses

Statistical analyses were conducted using R version 3.4.1 (The R Foundation, Vienna, Austria). The autogenerated representative values of R1, R2 and R1R2avg in each session were used in all statistical analyses. The data were expressed as group mean±SD. For all tests mentioned in the next paragraph, where applicable, P<0.05 was considered statistically significant.

First, the mean R1, R2 and R1R2avg were calculated for each breed. The absolute difference between R1 and R2, or $|\Delta(R1-R2)|$, was also calculated for each breed to evaluate the degree of

corneal astigmatism. Inter-breed variations in age, bodyweight, R1R2avg and |Δ(R1−R2)| were evaluated using Kruskal-Wallis tests. Pairwise comparisons using Bonferroni tests were further conducted to identify breed pairs with statistically significant differences between measurements when $P < 0.05$ was noted on Kruskal-Wallis tests. Spearman's correlation coefficient was calculated between R1R2avg and age, bodyweight, and |Δ(R1−R2)| for all data, regardless of the breed. Additionally, intra-breed variations in R1R2avg were evaluated for breeds with more than 10 dogs enrolled in the study. Spearman's correlation coefficient was calculated for each of these breeds between R1R2avg and age, bodyweight, and |Δ(R1−R2)|.

4.4   Results

Of the 974 dogs presented to the TUVMC during the study period, 381 were considered potential candidates for the study after they were evaluated according to criterion 1. Further screening of the dogs in terms of criteria 2 and 3 resulted in an enrolment of 299 dogs for keratometry examination. With regard to criterion 4, all these dogs were successful in providing measurements of both eyes. However, 23 dogs were excluded from the statistical analysis because the difference in R1R2avg between the right and left eyes was greater than 4.5% (mean±SD: 7.1±1.9%; range: 4.5–11.9). Finally, evaluation according to criterion 5 resulted in an exclusion of 39 dogs from 16 different breeds. This left a total of 474 corneas from 237 dogs (117 males and 120 females) of 16 different breeds for analysis. The algorithm for the inclusion and exclusion of dogs and the number of dogs which met or did not meet the criteria are shown in Figure 4-1. Age and bodyweight of all dogs

ranged from 0.8 to 16.9 (8.3±3.9) years old and from 1.2 to 45.0 (8.5±7.9) kg, respectively.

Table 4-1 summarises the descriptive statistics of signalment, bodyweight and keratometry of the 16 different breeds examined. The breed-specific mean of R1R2avg ranged from as small as 7.54±0.30 mm in Pomeranians to as large as 9.28±0.19 mm in Golden Retrievers and 9.28±0.39 mm in French Bulldogs. |Δ(R1−R2)| ranged from 0.22±0.11 mm in Miniature Schnauzers to 0.57±0.30 mm in French Bulldogs. Inter-breed variations in age, bodyweight, R1R2avg and |Δ(R1−R2)| evaluated using Kruskal-Wallis tests revealed P<0.01 for all variables. On further analysis using Bonferroni tests, significant differences in age were mostly identified when the breeds were compared against Miniature Dachshunds and Miniature Schnauzers (Table 4-1). Breed pairs identified to have significant differences in bodyweight and R1R2avg following Bonferroni tests are summarised in Table 4-2. The results revealed that Shih Tzus and French Bulldogs had an R1R2avg value similar to those of some other breeds with significantly heavier bodyweight (P<0.05). Shiba Inus and Shetland Sheepdogs were characterised by an R1R2avg value close to the breeds which weighed significantly less (P<0.05). With regard to |Δ(R1−R2)|, French Bulldogs had the largest value among all of the breeds evaluated, and a statistically significant difference was present when compared with six other breeds, as shown in Table 4-1. On evaluating the overall relationship between R1R2avg and bodyweight, Spearman's correlation coefficient revealed a relatively strong positive correlation between these two variables (r=0.72, P<0.01) (Figure 4-2a). However, both age and |Δ(R1−R2)| were poorly correlated with R1R2avg (r=0.18, P<0.01; r=0.08, P=0.09) (Figure 4-2b, c).

Intra-breed variations between R1R2avg and bodyweight and between R1R2avg and age

were analysed in the following seven breeds: Chihuahuas, Yorkshire Terriers, Toy Poodles, Miniature

Dachshunds, Beagles, Shiba Inus and Labrador Retrievers. Spearman's correlation coefficient

calculated for R1R2avg and bodyweight, as shown in Figure 4-3, revealed a relatively strong positive

correlation in Beagles (r=0.81, P<0.01), mild-to-moderate positive correlations in Toy Poodles and

Shiba Inus (r=0.64, P<0.01; r=0.61, P<0.01), and a weak positive correlation in Miniature

Dachshunds (r=0.38, P<0.01). No or little correlations were found in the other three breeds.

Evaluations between R1R2avg and age only identified weak to very weak positive correlations in

Labrador Retrievers and Miniature Dachshunds (r=0.39, P=0.03; r=0.33, P<0.01). Shiba Inus was the

only breed which was identified to have a weak positive correlation between R1R2avg and

|Δ(R1−R2)| (r=0.43, P=0.02). The rest of the breeds had no or little correlations between these

variables.

4.5 Discussion

The present study revealed considerable inter-breed variations in R1R2avg among the 16

studied breeds. Generally, R1R2avg showed a tendency to increase as the size of the dog increased,

but no such trend was identified between R1R2avg and age, or between R1R2avg and |Δ(R1−R2)|. In

other words, the shape of the cornea tended to be significantly rounder in smaller dogs and flatter in

larger dogs. Ageing and the degree of corneal astigmatism were not necessarily correlated with the

changes in corneal shape in dogs. This result was comparable with the trend reported by Gaiddon *et al*

[23], who compared measurements among small, medium and large dogs (8.09, 8.30 and 9.03 mm,

respectively). However, a closer examination of R1R2avg according to breed showed that some breeds did not follow this trend. Shiba Inus and Shetland Sheepdogs were characterised by smaller corneal curvatures than were other similarly weighing breeds such as Beagles and Welsh Corgis. Shih Tzus and French Bulldogs, in contrast, were found to have larger corneal curvatures comparable with those of Labrador Retrievers and Golden Retrievers. This result has important implications in the clinical setting, particularly when contact lenses are prescribed to dogs of various breeds for therapeutic purposes.

Similarly, this study found varying degrees of corneal astigmatism among the dog breeds examined, with statistically significant differences identified between French Bulldogs and six other breeds. The results indicated that the shape of the cornea of dogs varies significantly depending on breeds, from the cornea being ovoid to some degree as in French Bulldogs to that being more spherical as in Miniature Schnauzers and Beagles, for example. Some previous studies reported that mild astigmatism was common in dogs based on keratometry examinations [23], while others reported it being relatively uncommon based on retinoscopy examinations [76–77]. It is important to remember that corneal astigmatism noted with keratometry is based only on measurements of the anterior corneal curvature. It does not account for the effects of other structures such as the posterior corneal curvature, the lens and the axial length of the eye on visual consequences. Recent studies in humans revealed that the posterior corneal curvature effectively reduces total corneal astigmatism, partially compensating for anterior corneal astigmatism [78]. In dogs, it is quite possible that the posterior corneal curvature, together with other morphological and structural variations reported in the face and

the retina [79–81], may also vary between breeds, minimising the impact of inter-breed variations noted in the anterior corneal curvature on vision. However, none of the previous studies has particularly evaluated French Bulldogs to prove that this breed is not an exception. The finding in this study using a device that employs the mire ring principle is novel and could provide a new perspective for future optometric studies in dogs by describing reference values for anterior corneal astigmatism specific to some breeds.

Another point worth mentioning is that the correlation between R1R2avg and bodyweight of dogs of the same breed was inconsistent depending on the breed, while a relatively strong positive correlation was found when these were compared across breeds. Among the seven different breeds evaluated in the present study, good intra-breed correlation was found in Beagles, Shiba Inus and Toy Poodles, but not in Chihuahuas, Yorkshire Terriers, Miniature Dachshunds and Labrador Retrievers. This result could partly be related to the body condition score of the dogs enrolled in the study. Usui *et al* reported that Miniature Dachshunds and Chihuahuas were the top 2 breeds with the highest prevalence of obesity among many other dog breeds seen in private veterinary clinics in Japan [82]. Other factors such as lifestyle and social status of the owners, as well as the genetics of dogs, could have also contributed to the result. However, their impact could not be clearly determined in this study owing to the small sample size for each breed and due to limited information, including lack of information on body condition score of the studied dogs, for extensive evaluations, thus necessitating further investigations.

One of the major limitations of this study is the possible measurement errors associated with

the use of a handheld device on awake dogs. These errors were attributable either to the examiner due to instability of the hand holding the device or to the dogs due to poor vision fixation or headshaking due to, for example, panting. While such errors were difficult to completely eliminate, the reliability of the measurements taken in this study was maximised by employing the following measures. First, all measurements were obtained by a single trained examiner to eliminate possible inter-examiner variability. Intra-examiner variability of the data obtained by this examiner was minimised by conducting training sessions before the start of the study and was validated to be less than 4.5% based on a preliminary study using extracted porcine globes. Secondly, criterion 4 was set to eliminate data which fall outside the range explained by intra-examiner variability. It was considered that the data which did not meet criterion 4 might have been affected by poor animal cooperation. In the present study, all dogs which underwent keratometry examination successfully provided measurements of both eyes, while the threshold of 4.5% resulted in the removal of approximately 8% of dogs from further analyses. Although animal cooperation could become a source of measurement errors, feasibility of keratometry in awake dogs using the RKT was demonstrated in chapter 1. Additionally, a validity of over 90% achieved on the data taken from awake dogs of general population suggested that animal cooperation was not a major constraint to obtaining reasonably reliable measurements when performing keratometry using the device adopted in this study.

Other limitations of this study included those inherent to keratometers: (1) the area of the cornea measured using keratometers is limited to the central area 3–4 mm in diameter, which theoretically does not account for the shape of the cornea peripheral to this range; (2) the device is

pre-set to measure major and minor meridians at a right angle to each other assuming that the cornea has a symmetric spherical shape; thus, irregular astigmatism cannot be evaluated using keratometers; and (3) the distortion of the mire rings reflected on the corneal surface precludes the measurement, resulting in inaccuracy or failure in reading. These limitations need to be overcome by employing more sophisticated evaluation modalities, such as anterior-segment OCT and corneal topographers, if more accurate and comprehensive evaluations of the cornea are required, such as for correction of refractive error and evaluation of astigmatism following refractive surgery, as is often conducted in human ophthalmology.

In conclusion, the present study successfully described keratometry in 16 selected breeds of dogs which are popular in Japan using an automated handheld RKT. Only few reports have been published on keratometry in dogs [22–24, 30]. They generally discussed keratometry in dogs across several breeds involved in the studies, thus lacking detailed data regarding breed-specific keratometry. Devices which employ different measuring principles have advantages and disadvantages different from each other as partly described in chapter 2. Limitations associated with keratometry examinations in awake dogs included those attributable to examiners, animals and devices. In the present study, reliability of the data was improved by employing a single well-trained examiner and by adopting a device that employs the mire ring principle. The present study contributed to widening knowledge on keratometry in some breeds which had not been examined previously. The results also provided a valuable data set which could serve as a useful reference for breed-specific keratometry in normal dogs. Possible inter-examiner variability in the use of the device should be taken into

consideration when multiple examiners were involved in examinations. These results have

implications in determining therapeutic interventions, particularly in the treatment of various corneal

diseases using therapeutic contact lenses in dogs, as well as in exploring variations of canine corneal

topography by filling the knowledge gap for future research.

4.6 Tables and Figures

Table 4-1. Descriptive summary of signalment, bodyweight, and keratometry of the dogs enrolled in the study, according to breed. Breeds are listed in order of increasing mean bodyweight. Data are expressed as mean±SD, where applicable.

Breed	n (dogs)	Sex (M/F)	Age (years)	Bodyweight (kg)	R1 (mm)	R2 (mm)	R1R2avg (mm)	|Δ(R1-R2)| (mm)
Chihuahuas	26	17/9	8.2±4.1	3.2±1.0	8.06±0.34	7.66±0.33	7.86±0.32	0.41±0.21
Yorkshire Terriers	10	6/4	9.3±2.2	3.4±0.8	7.89±0.55	7.57±0.46	7.73±0.49	0.33±0.23
Pomeranians	6	2/4	7.1±4.9	3.5±1.2	7.70±0.40	7.38±0.23	7.54±0.30	0.32±0.27
Toy Poodles	44	21/23	6.6±3.8 [a, b]	4.1±1.6	7.99±0.38	7.68±0.39	7.84±0.38	0.31±0.21 [c]
Miniature Pinchers	5	4/1	9.4±4.3	4.5±1.2	7.98±0.25	7.63±0.23	7.81±0.23	0.34±0.10
Shih Tzus	7	3/4	5.8±3.1 [a, b]	5.5±0.6	9.20±0.48	8.68±0.40	8.94±0.43	0.52±0.24
Italian Greyhounds	7	2/5	9.0±2.9	5.6±0.6	8.44±0.35	8.16±0.39	8.30±0.36	0.28±0.18
Miniature Dachshunds	51	27/24	10.5±3.2	6.1±1.9	8.73±0.39	8.41±0.34	8.58±0.34	0.32±0.25 [c]
Miniature Schnauzers	5	4/1	11.6±2.1	8.5±1.5	8.56±0.31	8.34±0.28	8.45±0.29	0.22±0.11 [c]
French Bulldogs	9	1/8	7.0±3.4 [a]	9.3±2.2	9.56±0.45	9.00±0.38	9.28±0.39	0.57±0.30
Beagles	13	6/7	5.9±4.1 [a]	9.7±2.2	9.01±0.31	8.75±0.35	8.88±0.33	0.26±0.11 [c]
Shiba inus	16	10/6	6.7±3.4 [a, b]	9.8±2.0	8.32±0.48	7.93±0.39	8.13±0.40	0.39±0.36
Welsh Corgis	9	2/7	8.1±3.2	10.8±1.8	8.87±0.27	8.59±0.30	8.73±0.28	0.28±0.16 [c]
Shetland Sheepdogs	5	0/5	10.1±3.0	12.0±1.7	8.34±0.16	8.03±0.08	8.19±0.09	0.32±0.17
Labrador Retrievers	16	6/10	8.4±4.1	29.0±6.5	9.34±0.24	9.04±0.21	9.19±0.21	0.30±0.15 [c]
Golden Retrievers	8	6/2	10.3±3.1	30.3±7.0	9.45±0.24	9.12±0.17	9.28±0.19	0.33±0.15

M=male; F=female; R1=radius of the minor corneal meridian; R2=radius of the major corneal meridian; R1R2avg=mean of R1 and R2; |Δ(R1-R2)|=absolute difference between R1 and R2. [a] P<0.05 when compared with the mean age of Miniature Dachshunds (Bonferroni tests). [b] P<0.05 when compared with the mean age of Miniature Schnauzers (Bonferroni tests). [c] P<0.05 when compared with the mean |Δ(R1-R2)| of French Bulldogs (Bonferroni tests).

Table 4-2. Results of pairwise comparisons between the studied breeds using Bonferroni test with respect to bodyweight and mean radius of the corneal curvature (R1R2avg). Breeds are listed in order of increasing mean bodyweight. Breed pairs with statistically significant differences in either or both variables are shown.

Breed	Chihuahuas	Yorkshire Terriers	Pomeranians	Toy Poodles	Miniature Pinchers	Shih Tzus	Italian Greyhounds	Miniature Dachshunds	Miniature Schnauzers	French Bulldogs	Beagles	Shiba Inus	Welsh Corgis	Shetland Sheepdogs	Labrador Retrievers	Golden Retrievers
Chihuahuas	-															
Yorkshire Terriers		-														
Pomeranians			-													
Toy Poodles				-												
Miniature Pinchers					-											
Shih Tzus	◎	◎	◎	◎	●	-										
Italian Greyhounds	◎	○	●	◎		●	-									
Miniature Dachshunds	◎	◎	◎	◎	●			-								
Miniature Schnauzers	◎	○	◎	◎		○	○		-							
French Bulldogs	◎	◎	◎	◎	◎	○	◎	◎	●	-						
Beagles	◎	◎	◎	◎	◎	○	◎	◎			-					
Shiba Inus	◎	○	◎	◎	○	◎	○	◎		●	●	-				
Welsh Corgis	◎	◎	◎	◎	◎	○	○	○		●	●		-			
Shetland Sheepdogs	○	○	◎	○	○	◎	○	◎		●	●		●	-		
Labrador Retrievers	◎	◎	◎	◎	◎	○	◎	◎	◎	○	○	◎	◎	◎	-	
Golden Retrievers	◎	◎	◎	◎	◎	○	◎	◎	◎	○	◎	◎	◎	◎		-

◎=P<0.05 in both bodyweight and R1R2avg; ○=P<0.05 in bodyweight only (no significant differences in R1R2avg); ●=P<0.05 in R1R2avg only (no significant differences in bodyweight).
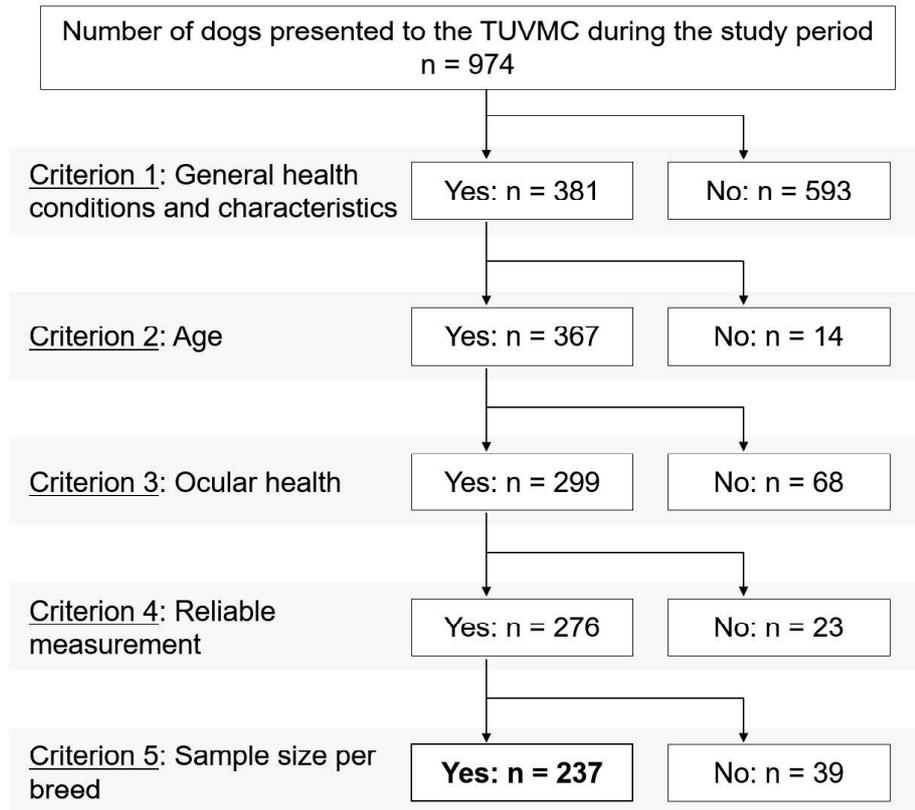
Figure 4-1. The algorithm for the inclusion and exclusion of dogs. The inclusion criteria were as follows: (1) the dog was clinically stable and could tolerate manual restraint of the head for thorough ophthalmic and keratometry examinations without sedation or general anaesthesia; (2) the dog was aged 10 months or older; (3) the dog had no ocular or periorbital diseases which could potentially affect ocular morphology or corneal conformations of both eyes; (4) both the right and left eyes were measured successfully and the difference in mean radius of the corneal curvature between the right and left eyes was less than 4.5%; and (5) data from more than five individuals per breed were available when the dogs were classified by breeds. TUVMC=Tottori University Veterinary Medical Centre.
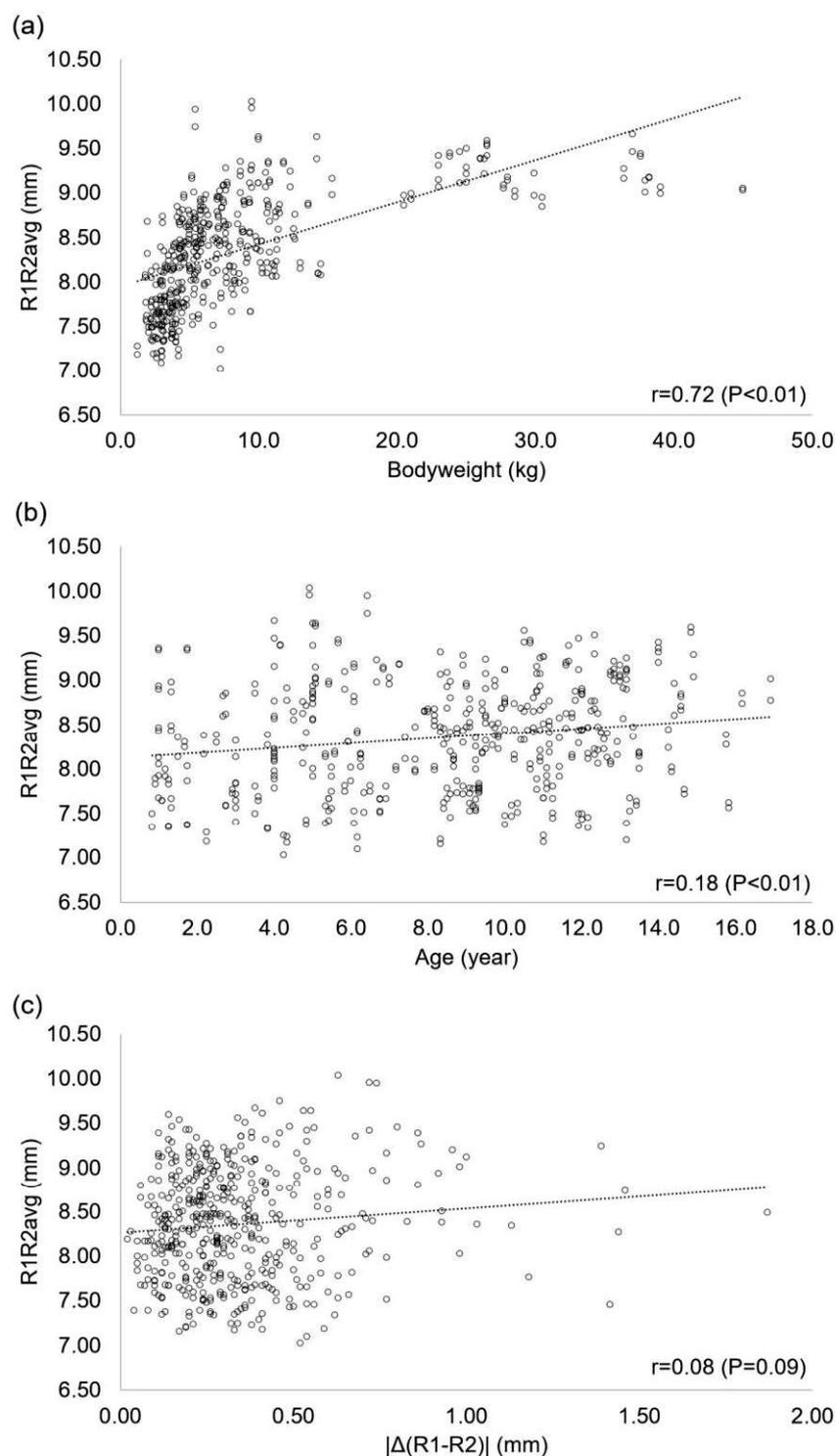
Figure 4-2. Scatter plots with a linear regression line showing the relationships (a) between bodyweight and R1R2avg, (b) between age and R1R2avg, and (c) between |Δ(R1−R2)| and R1R2avg of all dogs enrolled in the study (n=237 dogs). R1=radius of the minor corneal meridian; R2=radius of the major corneal meridian; R1R2avg=mean of R1 and R2; |Δ(R1−R2)|=absolute difference between R1 and R2.
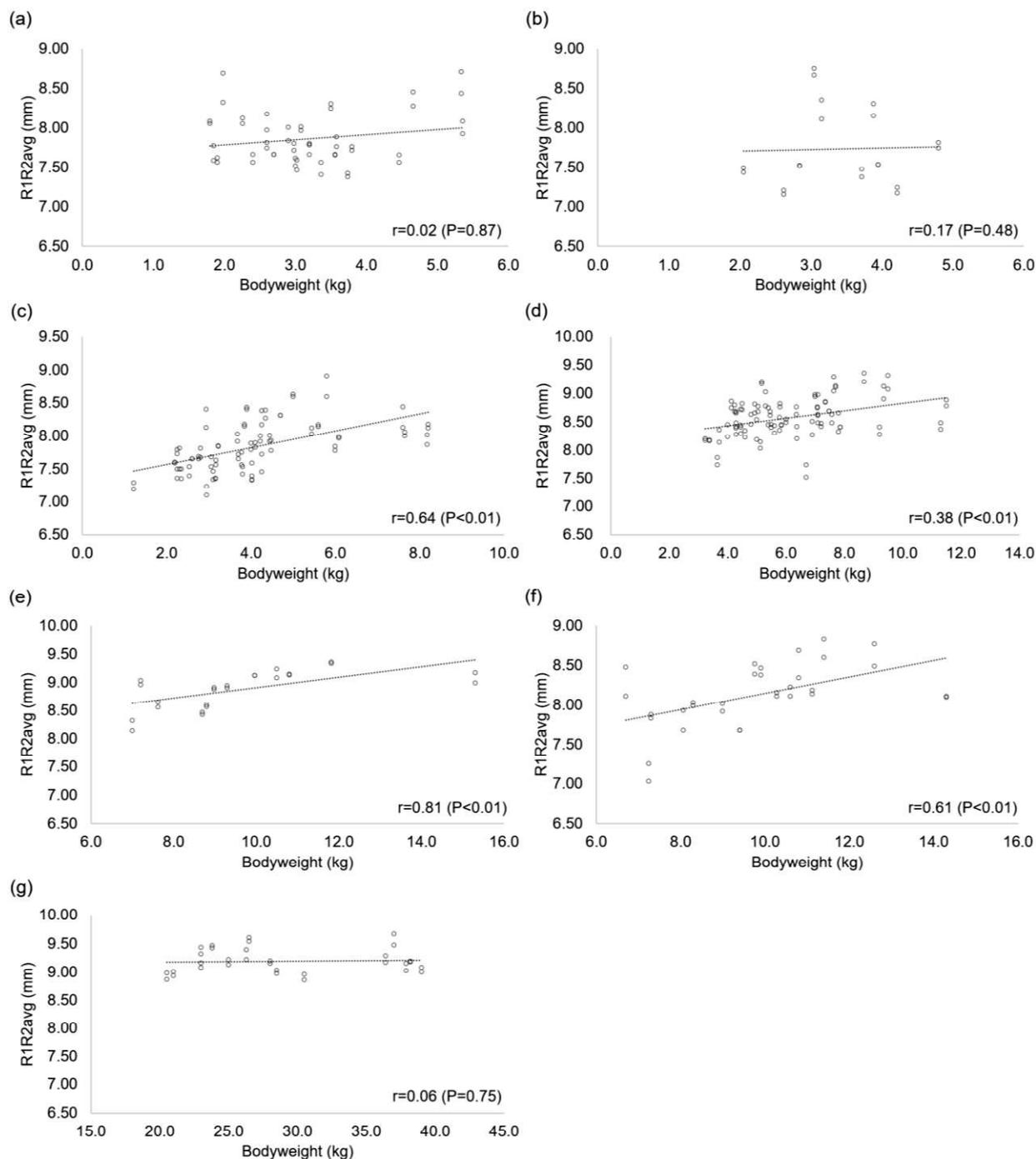
Figure 4-3. Scatter plots with a linear regression line showing intra-breed relationships between bodyweight and mean radius of the corneal curvature (R1R2avg) of the following seven breeds: (a) Chihuahuas (n=26), (b) Yorkshire Terriers (n=10), (c) Toy Poodles (n=44), (d) Miniature Dachshunds (n=51), (e) Beagles (n=13), (f) Shiba Inus (n=16) and (g) Labrador Retrievers (n=16).

CHAPTER 5

Keratometry in normal cats: a cross-sectional study in Japan using an automated

handheld keratometer

5.1 Abstract

Keratometry was performed in 73 domestic cats of varied signalment in Japan using an automated

handheld RKT. R1R2avg was significantly lower for cats younger than 1 year than for those older

than 2 years (8.04 mm vs. 8.80−8.99 mm, P<0.01). R1R2avg was significantly greater in males than

in females among the cats older than 11 years (9.22 mm vs. 8.84 mm, P=0.01), while the age

distributions of the males and females were similar. $|\Delta(R1\text{-}R2)|$ did not significantly differ across the

gender and age groups. The predictability of R1R2avg and $|\Delta(R1\text{-}R2)|$ was approximately 41−43%

and less than 3%, respectively, as a function of age and bodyweight. The results highlighted some

age- and sex-related keratometric variations in domestic cats in Japan.

5.2 Introduction

Keratometry, or the measurement of corneal curvature, is routinely performed in human

ophthalmology. It provides essential information for various clinical purposes such as the fitting of

contact lenses, diagnosing keratoconus, and planning refractive surgery. These applications, especially

the fitting of contact lenses for therapeutic purposes, have become increasingly popular in veterinary

ophthalmology. In cats, the use of bandage contact lenses has been reported in the management of various corneal diseases [9, 83–85]. While properly fitted contact lenses are safe and effective, poorly fitted ones often result in problems such as the premature detachment of the lens and the development of corneal oedema and neovascularization [9, 86]. Although keratometry is rarely utilized in veterinary clinical ophthalmology, it guides the estimation of the optimal base curve of a contact lens and facilitates the optimal fitting of contact lenses for patients.

Several studies have conducted keratometry for cats, as well as other evaluations of corneal morphology such as biometry and topography [25–26, 59, 87–90]. Most of these studies involved a small number of cats that were sourced from a closed breeding colony or a research population. Therefore, their results may have limited applicability to the general domestic cat population or other particular strains of cats seen at veterinary practices.

In humans, corneal curvature measurements show significant variations among different populations and across different sexes of the same nationality and race [91–93]. This was also evident when keratometry was performed for dogs of different breeds as described in chapter 4 and breed groups segregated by their body size [23]. In cats, these evaluations have not been conducted. Therefore, the degree of variations among different populations, if any, remains unknown. It is expected that investigating keratometry in cats with varied signalment will help to fill the current knowledge gap.

Previously, most of the studies involving cats were conducted under sedation. While it may be helpful to achieve an optimal corneal alignment for measurement, this necessitates the regular

application of artificial tears to prevent corneal desiccation. A study involving humans has demonstrated that the application of artificial tears and measurement in the lying posture have negative effects on the accuracy of keratometry [50]. Thus, it may be desirable to perform keratometry in cats in a sitting posture and without using sedation or general anaesthesia.

An automated keratometer can rapidly measure anterior corneal curvature. It is useful for the examination of human paediatric patients [31, 34] and has also been used in some studies for dogs and cats [22, 25–26, 30, 89]. Its applicability without sedation or general anaesthesia has been validated in dogs [22, 30], but it has not yet been evaluated in cats. Therefore, the present study aimed to assess the feasibility of keratometry in awake cats using an automated handheld RKT and to describe normative values for the radius of the anterior corneal curvature and corneal astigmatism, in a cross-section of the feline population in Japan. The keratometric values for different sexes and age groups were compared, and their associations with the age and bodyweight of cats were also evaluated.

5.3   Materials and Methods

Animals

The radii of the anterior corneal curvatures of 146 eyes of 73 privately owned cats of varied signalment were recorded. Prior to their enrolment in the study, they underwent thorough physical and ophthalmic examinations by veterinarians at the ophthalmology department at the TUVMC. The ophthalmic examinations included slit-lamp biomicroscopy (SL-17; Kowa, Tokyo, Japan), fluorescein

staining (FLUORES Ocular Examination Test Paper 0.7 mg; AYUMI Pharmaceutical Corp., Tokyo,

Japan), and applanation tonometry (Tono-Pen XL; Reichert, Depew, NY, US). Only those who were

clinically stable and free of ocular disease that could potentially affect corneal conformations in both

eyes were evaluated in this study. All aspects of the study were approved by the Animal Clinical

Research Ethics Committee of Tottori University (permission No.: H29-006). Full consent was

obtained from all cat owners using printed documents before examinations.

Procedures

Keratometry was performed using HandyRef-K (Nidek, Gamagoori, Japan), an automated

handheld RKT. R1 and R2, which represent the radii of the flattest and the steepest corneal curvatures,

respectively, were recorded for each eye. R1R2avg was calculated as the average of these two

measurements. The degree of corneal astigmatism ($|\Delta(R1-R2)|$) was also calculated as the absolute

difference between R1 and R2 in dioptres. All the measurements were obtained by a single examiner

following the technique described in chapter 1. At least three consecutive measurements were

obtained for each eye, and the averages of these measurements were used for statistical analysis.

Statistical Analyses

The statistical analyses were performed using R version 3.4.1 (The R Foundation, Vienna,

Austria). At first, the measurements of the right and left eyes were compared using the Wilcoxon

signed-rank test. Because there was no significant difference between these measurements, the mean

keratometric value for each animal, based on the measurements from pairs of right and left eyes, was

used in the subsequent analyses. The cats were then classified into two groups according to their sex

(male or female). The group means and medians for the measured variables were derived for the groups and compared using the Mann-Whitney U test. The cats were reclassified into five groups according to their age (less than 1 year old, 1−2 years old, 3−6 years old, 7−10 years old, and 11 years old or older). The Kruskal-Wallis test was used to compare the group medians of the measured values for the various age groups. Regression analysis using a least-squares method was used to evaluate the relationships between age and R1R2avg, bodyweight and R1R2avg, age and $|\Delta(R1-R2)|$, and bodyweight and $|\Delta(R1-R2)|$. The data were expressed as group medians unless otherwise indicated. P-values of <0.05 were considered statistically significant.

5.4   Results

The cats evaluated in this study included 39 males and 34 females. Mixed-breed cats accounted for 78% of the study population. There were 12 pure breeds, with a few individuals belonging to each. These included American Shorthairs, British Shorthair, Chartreux, Chinchilla, Maine Coon, Munchkin, Norwegian Forest Cat, Persians, Ragdoll, Scottish Folds, Selkirk Rex, and Siberian. The age of the cats ranged from 2 months to 18 years old (mean±SD: 6.9±5.4; median: 5.5). The bodyweight of the cats ranged from 0.8 to 7.8 kg (3.8±1.3; 3.6). The male cats were significantly younger but heavier than the female cats (median age: 4.0 years old vs. 8.3 years old, P=0.01; bodyweight: 4.1 kg vs. 3.1 kg, P<0.01).

The measurements of the right and left eyes were not statistically different (P=0.2−0.3) (Table 5-1). The overall mean of R1R2avg was 8.82±0.49 mm (median: 8.85), with a range of

6.77−9.78 mm. The mean of $|\Delta(R1-R2)|$ of all cats was 1.16±0.83 dioptres (1.00), with a range of 0.00−4.75 dioptres.

The corneas of the male cats were significantly flatter than those of the female cats (P<0.01) (Table 5-2). $|\Delta(R1-R2)|$ in the males and females were not significantly different (P=0.85). The cats younger than 1 year consisted of small but almost an even number of males and females (male/female=5/4). In this group of cats, the median age and R1R2avg were lower in the males than in the females (Table 5-3). The differences in these variables across the sexes were not statistically significant (P=0.28 and 0.29). R1R2avg of the cats in this age group was significantly lower than those of the other age groups (8.04 mm vs. 8.80−8.99 mm, P<0.01). R1R2avg of the cats aged 11 years or older was significantly greater in males than in females (9.22 mm vs 8.84 mm, P=0.01), while the median age of the cats did not differ with sex (13.0 years vs 14.0 years, P=0.38) (Table 5-3). R1R2avg for the four age groups that had cats older than 1 year were not different (P=1.0). $|\Delta(R1-R2)|$ in the age groups were also not different (0.69−1.38 D, P=0.43).

The overall relationship between age and R1R2avg is shown in Figure 5-1. In general, R1R2avg was best fitted with a logarithmic curve. The general formula obtained in this study to predict R1R2avg of the cats of different ages was as follows: R1R2avg=A * ln (X) + B, where R1R2avg is the mean radius of the corneal curvature in mm, X is the age of a cat in years, and A and B are constants. For the overall population, A and B were determined as 0.2721 and 8.4137, respectively. The predictability of R1R2avg obtained with this formula was approximately 43% (R^2=0.43). The scatter plot revealed that R1R2avg of the adult male cats was generally greater than

that of the adult female cats (Figure 5-1a). This trend was observed among the cats aged 1.3 years or older according to the regression curves drawn separately for male and female cats.

Higher predictability was achieved when the curve was fitted for the population of cats younger than 3 years (R^2=0.72) (Figure 5-1b). The predictive formula for this population was defined with the following constants: A=0.605 and B=8.4458. The formula for the population of cats older than 3 years used the following constants: A=0.0733 and B=8.8083. However, the coefficient of determination of this formula was very low (R^2=0.02), indicating that R1R2avg cannot be predicted reliably in this group of cats due to a relatively high variation among individuals. Nonetheless, the predicted R1R2avg of the adult cats reached a plateau of 9.0 mm at the age of 7 years and for up to 20 years, based on this formula.

Figure 5-2 shows the relationship between bodyweight and R1R2avg, which was also best fitted with a logarithmic curve. R1R2avg of the cats was predicted using the following formula as a function of bodyweight: R1R2avg=A * ln (X) + B, where R1R2avg is the mean corneal curvature radius in mm, X is the bodyweight of a cat in kg, and A and B are constants. For the overall population, A and B were determined as 0.8414 and 7.7393, respectively. The predictability of R1R2avg using this formula was approximately 41% (R^2=0.41). The general trend observed on the scatter plot was not different for males and females.

The overall relationship between age and $|\Delta(R1-R2)|$ is shown in Figure 5-3. In general, $|\Delta(R1-R2)|$ fitted poorly with any line or curve, indicating low predictability as a function of both age and bodyweight (R^2=0.03 and 0.01). The scatter plot did not reveal different trends for male and

female cats.

5.5 Discussion

This study documented the radius of the anterior corneal curvature and corneal astigmatism in a cross-section of the normal domestic cats in Japan. The measurements were obtained successfully for both the right and left eyes of all cats enrolled in the study. The keratometry was well-tolerated by all cats. A close agreement between the measurement for the pairs of right and left eyes in this study was consistent with previous findings [25–26, 59, 88–89]. The result indicated that keratometry was feasible in awake cats regardless of their age using the automated handheld RKT. This is especially important when considering the clinical application of keratometry, as not all feline patients are good candidates for sedation or general anaesthesia depending on their general health condition. The major advantages of the device used in this study include its ability to rapidly and consecutively record multiple measurements without direct contact with the corneal surface and to measure multiple variables at a time. This includes both the minor and major corneal curvatures and corneal astigmatism. These features minimise the stress exerted on cats and the risks of compression artefacts as well as the spread of infections that can result from the direct corneal contact during the measurement.

R1R2avg in cats aged 1 year or older in this study was generally greater than the value reported previously for adult cats and obtained using manual or automated keratometers and a Scheimpflug system (between 8.58 and 8.79 mm) [25–26, 59, 88–90]. The only study that reported a

relatively high value of 9.13 mm used a photokeratoscope [87]. The inconsistent results of these studies may have been related to the differences in cat signalment such as breed, sex, or age. While the domestic shorthair was the most common breed evaluated in the previous studies, the age and sex of the cats were not specified. Therefore, the results cannot be compared in this regard. The results may also have been influenced by the differences in the measuring technique or the device used [51, 74–75, 94]. Further studies are needed to investigate the factors that potentially affect the results of keratometry.

The present study found that R1R2avg increased logarithmically with time in young cats aged less than 3 years and reached a plateau later in their life. The trend was similar to that described by Freeman and Moodie *et al* [26, 59]. They independently suggested a formula to predict the corneal curvatures of young cats as a function of age based on the examination of kittens aged less than 35 weeks old and up to 67 weeks old, respectively. The predicted values according to their formulas were similar, yet they tended to be lower and reached a plateau at a younger age than that predicted by the formula reported in this study. This may be attributed to the generally flatter cornea of the cats in this study than those in previous studies, regardless of their age. Previously, it was suggested that the development of the feline cornea continues until approximately 18 months of age [26]. However, the result of this study suggests that the corneas of cats continue to develop or change shape until a much older age, although the extent of changes observed in adult cats is far lower than that in young cats.

Additionally, the present study documented a paradoxically greater R1R2avg in male cats than in female cats when the median age of the male cats tended to be lesser than that of the female

cats. This trend was consistently observed across all age groups of cats older than 1 year. This study was not designed to take age-matched samples from different sexes. This limitation may have affected the ability to make reasonable comparisons of the groups. Nevertheless, the result would provide an important implication for further investigations by potentially highlighting a previously undescribed feature of the feline cornea. The corneas of male cats are generally flatter than those of female cats when they get older than 1 year of age and especially in those aged 11 years or older. Interestingly, while the trend is inconsistent with the feature described in dogs [22–23], it aligned with the feature described in humans [91, 93]. This study involved a limited number of pure-breed cats. Therefore, the breed-related differences were not considered in this study although they could have also influenced the results. Further studies involving a wider range of age-matched cats, with more pure-breeds, are required to validate these findings.

$|\Delta(R1-R2)|$ of the cats evaluated in this study were generally greater than those of the adult cats reported in most studies (between 0.3 and 0.6 dioptres) [25, 87–89]. The use of different measuring techniques may have influenced the result. Previous studies determined corneal astigmatism based on the difference between the corneal curvatures measured along the vertical and horizontal axes [25–26, 59, 88–90]. Our study based the degree of astigmatism on the difference between the flattest and steepest corneal axes, which were not necessarily the vertical and horizontal axes. Thus, a larger value was expected in this study. The present results may be more accurate than the previous findings. Earlier studies also reported a decreasing trend in $|\Delta(R1-R2)|$ from less than 4 dioptres in young kittens to less than 1 dioptre in adult cats [26, 59]. However, this trend was not

observed in this study; an increasing trend was rather observed with increasing age. Detailed studies

on the axis of corneal astigmatism will be of value in explaining these differences.

In conclusion, this is the first cross-sectional study on keratometry for the domestic cat

population in Japan. An automated handheld keratometer is a useful tool for rapidly performing

keratometry in awake cats. The keratometric values obtained in this study were generally greater than

those in previous reports, suggesting that there may be some variations related to cat signalment. The

limitations associated with the study design leave room for further studies to validate the results.

These include the evaluation of the possible inter-examiner variability when multiple examiners were

involved in examinations. Nonetheless, the present data will be valuable contributions to the current

clinical and scientific knowledge of feline keratometry. Variations in R1R2avg among different cat

populations have important implications for making appropriate clinical decisions for each patient,

especially when therapeutic interventions are considered for various corneal diseases.

5.6   Tables and Figures

Table 5-1. Keratometric values for both eyes in 73 cats.

Eye	Mean±SD			Median (Minimum, Maximum)		
	Right	Left	Combined	Right	Left	Combined
R1 (mm)	8.94±0.54	8.97±0.52	8.95±0.53	8.95 (6.82, 10.17)	9.00 (7.20, 10.31)	8.98 (6.82, 10.31)
R2 (mm)	8.66±0.48	8.69±0.44	8.68±0.46	8.73 (6.72, 9.43)	8.74 (6.93, 9.57)	8.74 (6.72, 9.57)
R1R2avg (mm)	8.80±0.50	8.83±0.47	8.82±0.49	8.83 (6.77, 9.70)	8.86 (7.07, 9.78)	8.85 (6.77, 9.78)
|Δ(R1-R2)| (D)	1.19±0.85	1.14±0.82	1.16±0.83	1.00 (0.00, 4.75)	1.00 (0.00, 4.25)	1.00 (0.00, 4.75)

R1=radius of the minor corneal meridian; R2=radius of the major corneal meridian; R1R2avg=mean

of R1 and R2; |Δ(R1−R2)|=absolute difference between R1 and R2 in dioptres.

Table 5-2. Keratometric values of 73 cats segregated by sex (male: n=39; female: n=34).

	Mean±SD		Median (Minimum, Maximum)	
	Male	**Female**	**Male**	**Female**
R1 (mm)	9.01±0.58	8.88±0.45	9.03 (7.01, 9.86)	8.82 (7.91, 10.15)[a']
R2 (mm)	8.74±0.52	8.61±0.34	8.88 (6.83, 9.24)	8.59 (7.83, 9.43)[a']
R1R2avg (mm)	8.88±0.54	8.75±0.39	8.96 (6.92, 9.52)	8.68 (7.87, 9.71)[a']
|Δ(R1-R2)| (D)	1.16±0.73	1.17±0.67	1.00 (0.00, 3.50)	1.00 (0.38, 3.13)

R1=radius of the minor corneal meridian; R2=radius of the major corneal meridian; R1R2avg=mean of R1 and R2; |Δ(R1−R2)|=absolute difference between R1 and R2 in dioptres. [a'] $P<0.01$ when compared between male and female cats.

Table 5-3. Age and the mean radius of the corneal curvature of 73 cats segregated by age and sex.

	N (cats)	Age (years)		R1R2avg (mm)	
	Male/Female	Male	Female	Male	Female
<1 year old	5/4	0.4 (0.2, 0.9)	0.5 (0.4, 0.5)	7.86 (6.92, 8.80)	8.28 (7.87, 8.44)
1-2 years old	9/5	2.0 (1.2, 2.5)	2.8 (1.5, 2.9)[a']	8.89 (8.61, 9.49)	8.64 (8.23, 8.80)[a]
3-6 years old	11/7	4.7 (3.0, 6.2)	6.2 (3.0, 6.9)[a]	8.91 (8.60, 9.39)	8.76 (8.40, 9.54)
7-10 years old	6/7	9.3 (7.3, 10.3)	10.0 (9.7, 10.8)[a]	9.10 (8.81, 9.29)	8.75 (8.64, 9.56)
≥11 years old	8/11	13.0 (11.2, 17.0)	14.0 (11.2, 18.0)	9.22 (8.84, 9.52)	8.84 (8.50, 9.71)[a']

N=number of cats examined; R1R2avg=mean of R1 (radius of the minor corneal meridian) and R2 (radius of the major corneal meridian). Data are expressed as median and figures in brackets indicate minimum and maximum values, where applicable. [a] $P<0.05$ and [a'] $P<0.01$ when compared between male and female cats.

(a)

(b)
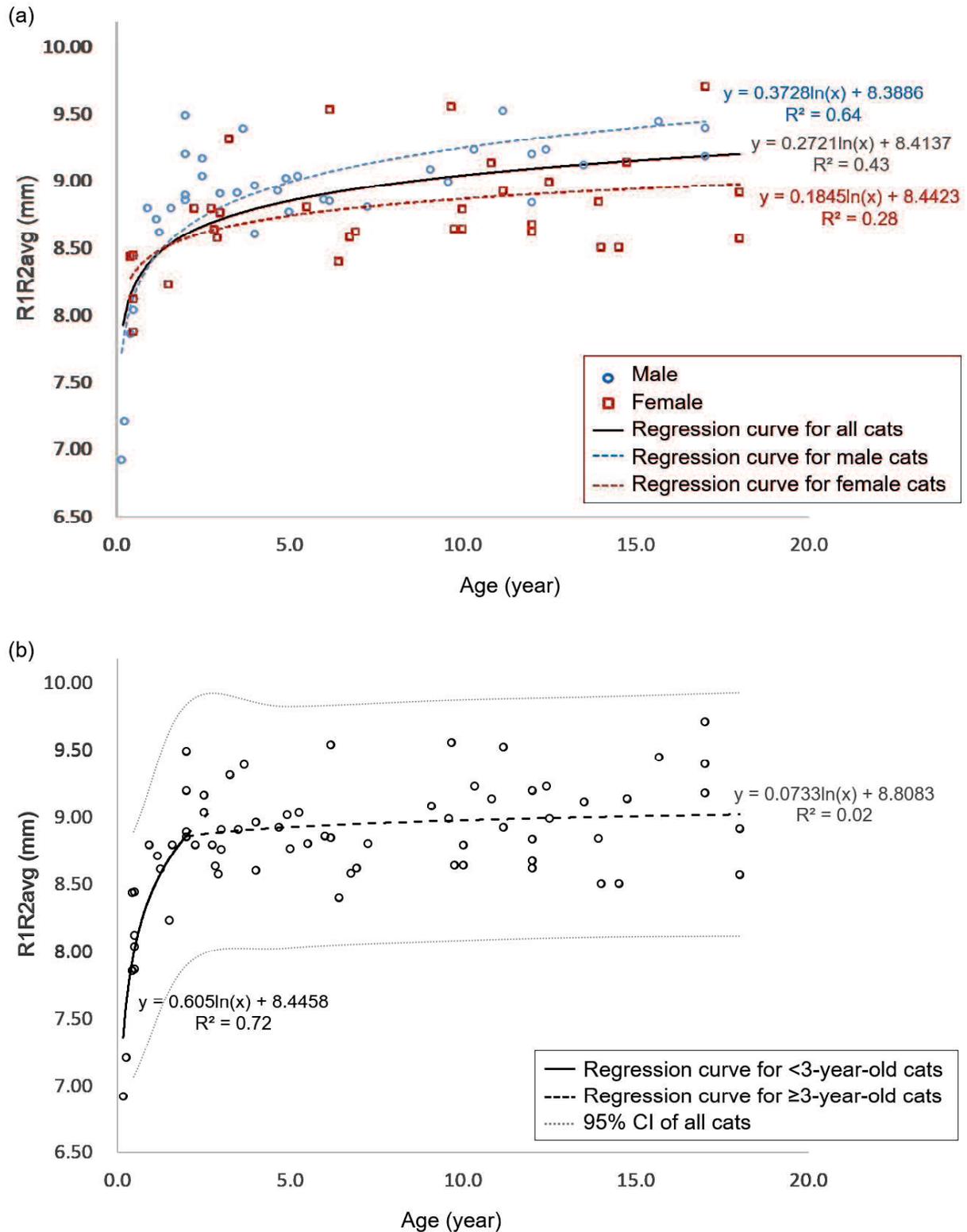
Figure 5-1. Mean radius of the corneal curvature (R1R2avg) of 73 cats as a function of age. The regression curves are fitted to the data segregated by (a) sex and (b) age. The 95% confidence intervals (CIs) are calculated based on the regression curves.
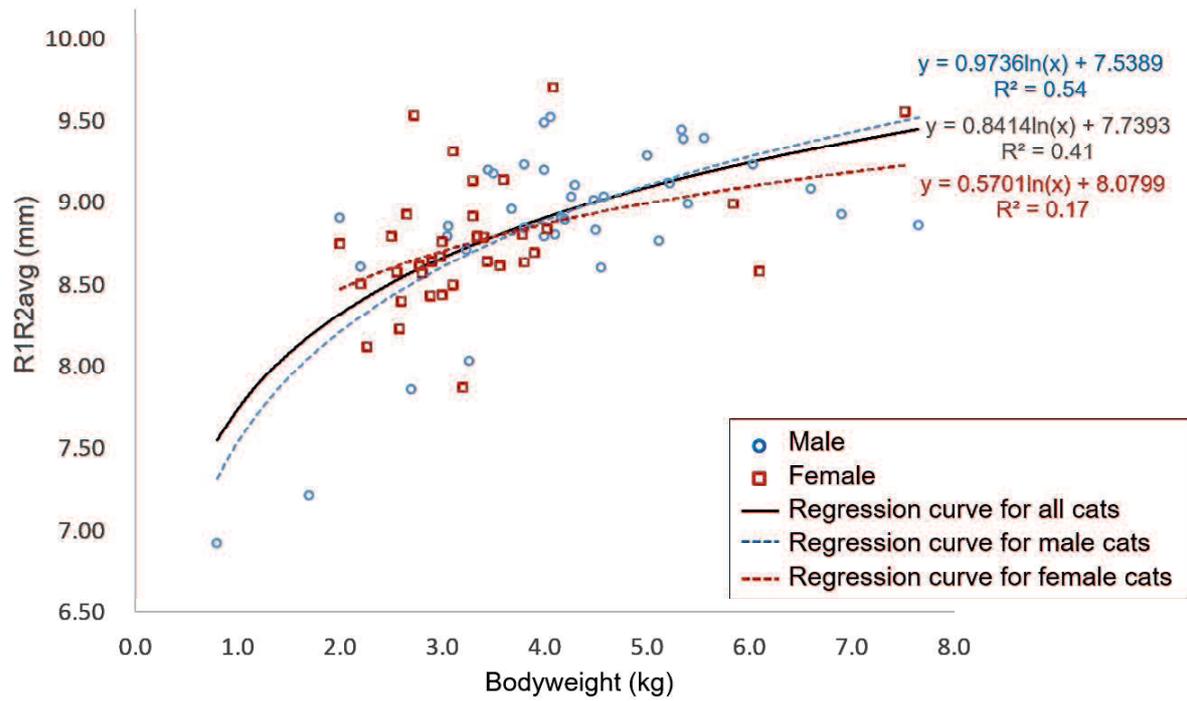
Figure 5-2. Mean radius of the corneal curvature (R1R2avg) of 73 cats as a function of bodyweight.

The regression curves are fitted to the data segregated by sex.
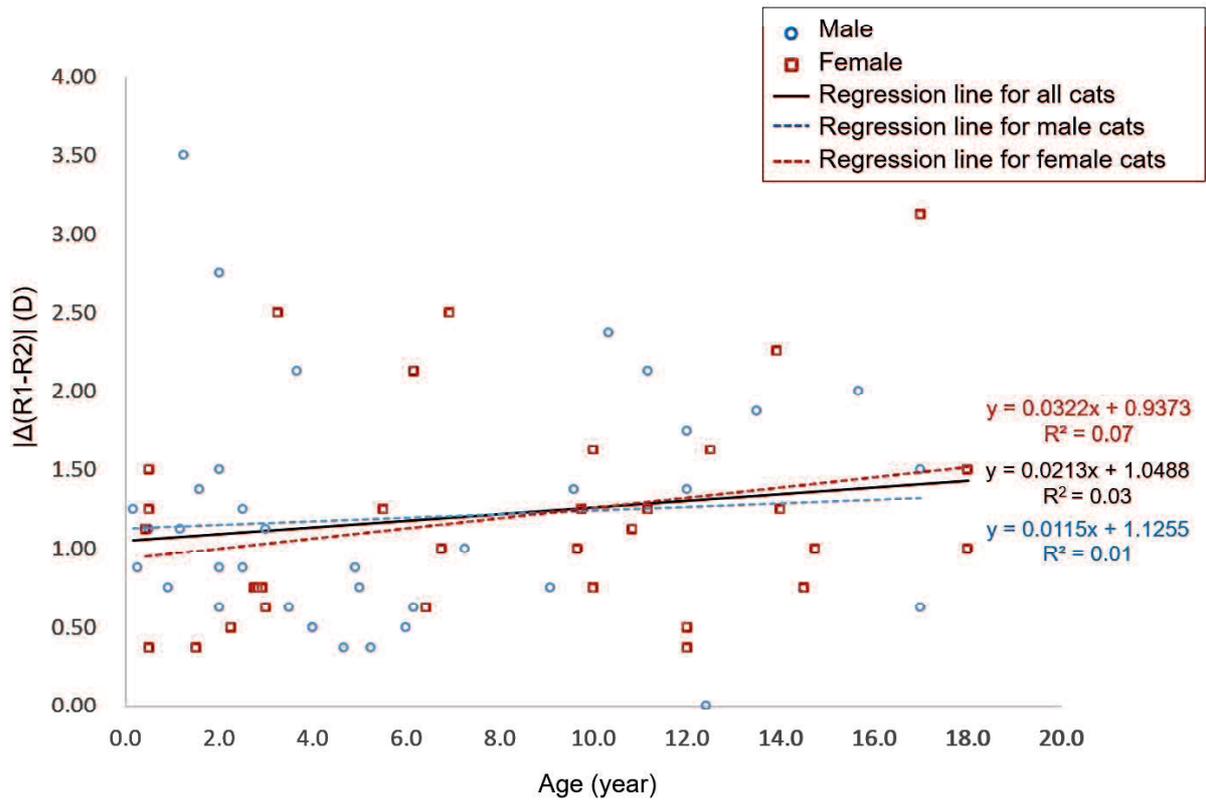
Figure 5-3. Degrees of corneal astigmatism ($|\Delta(R1-R2)|$) of 73 cats as a function of age. The regression lines are fitted to the data segregated by sex.

GENERAL CONCLUSION

This study was driven by the lack of detailed knowledge regarding corneal topography and keratometry in dogs and cats of varied signalment. The primary interest of this study was to describe normal keratometric values, including mean radius of the corneal curvature and corneal astigmatism, of dogs and cats which are popular in Japan using an automated handheld RKT. The study also investigated applicability of the RKT and OCT in awake dogs, and assessed interchangeability of different devices such as RKT, OCT, and US in keratometry in dogs. Additionally, the study evaluated corneal topography of dogs and cats using HCLs and assessed its association with the RKT readings.

In chapter 1, the study compared the keratometric values of laboratory beagles which were taken with and without sedation on two different days using the RKT and OCT. The results generally showed good agreement between the measurements taken at different sessions regardless of the use of sedation, indicating that both RKT and OCT can be used in awake dogs without causing clinically significant variations in the measurements.

In chapter 2, the keratometric values of laboratory beagles taken with three different devices, or RKT, OCT, and US, were compared to evaluate their interchangeability. The results showed considerable inter-device variations except between the measurements taken with the RKT, OCT at 10 mm diameter, and US at 12 mm diameter. Furthermore, the results showed an increasing trend in mean radius of the corneal curvature with increasing corneal diameter when measured by OCT and US. These results indicated that the measurements taken by different devices or at different diameters

need to be interpreted with caution, thus had clinically important implication.

In chapter 3, the shape of the anterior cornea of laboratory beagles and mixed-breed cats was determined based on the base curve of a parallel-fitting HCL with varying lens diameters. The results showed that the cornea of dogs and cats evaluated in this study were steeper centrally and became flatter toward periphery, as demonstrated by the OCT and US in chapter 2. The mean radius of the corneal curvature measured by RKT showed better agreement with the best-fit base curve of 8–10 mm diameter HCLs. The result indicated that the RKT reading reflected the curvature of more peripheral cornea of dogs and cats than that specified by the manufacture.

In chapter 4, the study described keratometry in 16 dog breeds using the RKT. Considerable inter-breed variations were noted in both mean radius of the corneal curvature and corneal astigmatism. In general, mean radius of the corneal curvature of dogs had positive correlation with their bodyweight. However, some breeds did not follow this trend and had relatively smaller or larger corneal curvatures than other similarly weighing breeds did. Mean radius of the corneal curvature of dogs did not correlated with their age nor with the corneal astigmatism. Intra-breed variations of the mean radius of the corneal curvature and the corneal astigmatism showed inconsistent associations with bodyweight of dogs depending on breeds. Breed-specific keratometry values described in this study provided clinically useful reference data which are important in various therapeutic interventions, such as fitting of therapeutic contact lenses, in different dog breeds.

In chapter 5, the study described keratometry of domestic cats using the RKT, with a particular interests in revealing associations between keratometry and cats' signalment. As in dogs, the

results showed a positive correlation between mean radius of the corneal curvature of cats and their bodyweight. The mean radius of the corneal curvature tended to be greater in males than in females. Moreover, it was significantly smaller in cats younger than 1 year than in those older than 2 years. Significant difference was not noted among cats older than 2 years. Corneal astigmatism was not different between males and females and between different age groups. The results highlighted some age- and sex-related variations in the mean radius of the corneal curvature in domestic cats which are popular in Japan.

In conclusion, both RKT and OCT used in this study were applicable for keratometry in awake dogs, and were capable of providing much stable measurements than US did. Interchangeable use of different devices is not recommended in patient monitor due to considerable inter-device variations. An increasing trend in the corneal curvature radius with increasing corneal diameter, as noted in laboratory beagles and mixed-breed cats, suggests that the measurements be taken at particular diameter of interest according to the purpose. It is worth noting that the measurements taken by the RKT are likely to represent the true corneal curvature radius at 8–10 mm diameters based on a HCL fitting. The present study also described details of keratometric values, including mean radius of the corneal curvature and the corneal astigmatism, in dogs and cats which are popular in Japan using the RKT, with respect to their signalment. The results succeeded to characterise the features of canine and feline corneas, and to provide valuable datasets which were useful both clinically and scientifically by filling the current knowledge gap around this area. The results are especially important clinically as breed- and species-specific keratometry of dogs and cats provides objective

guidance for selection and development of optimum contact lens specification, which has not been available previously. The results presented in this dissertation contributed to improve our understanding of canine and feline corneal topography and keratometry. This study also contributed to pave the way for further clinical and non-clinical studies on the use of keratometry for treatment of various corneal diseases and for various optometric studies.

<u>ACKNOWLEDGEMENTS</u>

<u>REFERENCES</u>

1. Douthwaite, W. A. and Evardson, W. T. 2000. Corneal topography by keratometry. *Br J Ophthalmol*. **84**: 842–847.

2. McMullen, R. J. Jr. and Gilger, B. C. 2006. Keratometry, biometry and prediction of intraocular lens power in the equine eye. *Vet Ophthalmol*. **9**: 357–360.

3. Ramakrishnan, R. and Naik, A. 2014. Comparison of manual keratometer with autokeratometer. *Biosci Biotechnol Res Asia.* **11**: 339–341.

4. Punjabi, S. and Bedi, N. 2016. A clinical study to evaluate therapeutic efficacy of soft contact lenses in corneal diseases. *Int J Res Med Sci*. **4**: 4632–4636.

5. Mashige, K. P. 2013. A review of corneal diameter, curvature and thickness values and influencing factors. *S Afr Optom*. **72**: 185–194.

6. Hashemi, H., Yekta, A., Ostadimoghaddam, H., Norouzirad, R. and Khabazkhoob, M. 2014. Comparison of keratometric values using Javal keratometer, Oculus Pentacam, and Orbscan II. *Iran J Ophthalmol*. **26**: 3–10.

7. Yeung, K. K., Silverman, B. S. and Kageyama, J. Y. 2001. Aphakic hydrogen contact lens fitting on a monocular canine: a case report. *Optometry*. **72**: 421–425.

8. Schmidt, G. M., Blanchard, G. L. and Keller, W. F. 1977. The use of hydrophilic contact lenses in corneal diseases of the dog and cat: a preliminary report. *J Small Anim Pract*. **18**: 773–777.

9. Bossuyt, S. M. 2016. The use of therapeutic soft contact bandage lenses in the dog and the cat: a series of 41 cases. *Vlaams Diergeneeskd Tijdschr.* **85**: 343–348.

10. Gosling, A. A., Labelle, A. L. and Breaux, C. B. 2013. Management of spontaneous chronic corneal epithelial defects (SCCEDs) in dogs with diamond burr debridement and placement of a bandage contact lens. *Vet Ophthalmol.* **16**: 83–88.

11. Woof, P. J. and Norman, J. C. 2015. Effect of corneal contact lens wear on healing time and comfort post LGK for treatment of SCCEDs in Boxers. *Vet Ophthalmol.* **18**: 364–370.

12. Grinninger, P., Verbruggen, A. M. J., Kraiger-Huver, I. M. G., Djajadiningrad-Laanen, S. C., Teske, E. and Boeve, M. H. 2015. Use of bandage contact lenses for treatment of spontaneous corneal epithelial defects in dogs. *J Small Anim Pract.* **56**: 446–449.

13. Dees, D. D., Fritz, K. J., Wagner, L., Paglia, D., Knollinger, A. M. and Madsen, R. 2017. Effect of bandage contact lens wear and postoperative medical therapies on corneal healing rate after diamond burr debridement in dogs. *Vet Ophthalmol.* **20**: 382–389.

14. Denk, N., Fritschet, J. and Reese, S. 2011. The effect of UV-blocking contact lenses as a therapy for canine chronic superficial keratitis. *Vet Ophthalmol.* **14**: 186–194.

15. Nevile, J. C., Hurn, S. D., Turner, A. G. and Morton, J. 2006. Diamond burr debridement of 34 canine corneas with presumed corneal calcareous degeneration. *Vet Ophthalmol.* **19**: 305–312.

16. Wada, S., Yoshinari, M. and Mizuno, Y. 2000. Practical usefulness of a therapeutic soft contact lens for a corneal ulcer in a racehorse. *Vet Ophthalmol.* **3**: 217–219.

17. Lassaline-Utter, M., Cutler, T. J., Michau, T. M. and Nunnery, M. M. 2014. Treatment of nonhealing corneal ulcers in 60 horses with diamond burr debridement (2010-2013). *Vet Ophthalmol.* **17**: 76–81.

18. Kecova, H. and Necas, A. 2004. Phacoemulsification and intraocular lens implantation: recent trends in cataract surgery. *Acta Vet Brno.* **73**: 85–92.

19. Mouney, M. N., Townsend, W. M. and Moore, G. E. 2012. Association of height, body weight, age, and corneal diameter with calculated intraocular lens strength on adult horses. *Am J Vet Res.* **73**: 1977–1982.

20. Townsend, W. M., Wasserman, N. and Jacobi, S. 2013. A pilot study on the corneal curvatures and ocular dimensions of horses less than one year of age. *Equine Vet J.* **45**: 256–258.

21. Badial, P. R., Cisneros-Alvarez, L. E., Bandao, C. V. S., Ranzani, J. J. T., Tomaz, M. A. R. V., Machado, V. M. and Borges, A. S. 2015. Ocular dimensions, corneal thickness, and corneal curvature in quarter horses with hereditary equine regional dermal asthenia. *Vet Ophthalmol.* **18**: 385–392.

22. Dixon, C. J. 2014. Keratometry of the canine cornea: preliminary findings of a cross-sectional study. In: Abstracts: Annual scientific meeting of the European college of veterinary ophthalmologists, London, UK May 15-18, 2014. *Vet. Ophthalmol.* **17**: E16–E30.

23. Gaiddon, J., Rosolen, S. G., Steru, L., Cook, C. S. and Peiffer, R. Jr. 1991. Use of biometry and keratometry for determining optimal power for intraocular lens implants in dogs. *Am J Vet Res.* **52**: 781–783.

24. Kudou, S. 1997. Study of lamellar corneal transplantation in dogs and cats. PhD Thesis, Azabu

    University.

25. Gilger, B. C., Davidson, M. G. and Howard, P. B. 1998. Keratometry, ultrasonic biometry, and

    prediction of intraocular lens power in the feline eye. *Am J Vet Res.* **59**: 131–134.

26. Moodie, K. L., Hashizume, N., Houston, D. L., Hoopes, P. J., Demidenko, E., Trembly, B. S. and

    Davidson, M. G. 2001. Postnatal development of corneal curvature and thickness in the cat. *Vet*

    Ophthalmol. **4**: 267–272.

27. Roth, N. 1969. Relationship between corneal radius of curvature and age in rabbits. *Br Vet J.* **125**:

    560–563.

28. Yuksel, H., Turkcu, F. M., Ari, S., Cinar, Y., Cingu, A. K., Sahin, M., Sahin, A., Ozkurt, Z. and

    Caca, I. 2015. Anterior segment parameters of rabbits with rotating Scheimpflug camera. *Vet*

    Ophthalmol. **18**: 210–213.

29. Murphy, C. J., Kern, T. J. and Howland, H. C. 1992. Refractive state, corneal curvature,

    accommodative range and ocular anatomy of the Asian elephant (*Elephas maximus*). *Vision Res.*

    32: 2013–2021.

30. Gorig, C., Meyer-Lindenberg, A., Ulrich, S., Wagner, F. and Nolte, I. 1997. Keratometry in dogs:

    comparison of two automatic hand-held keratometers. *Tierarztl Prax.* **25**: 659–665.

31. Harvey, E. M., Miller, J. M. and Dobson, V. 1995. Reproducibility of corneal astigmatism

    measurements with a hand held keratometer in preschool children. *Br J Ophthalmol.* **79**:

    983–990.

32. Wassill, K. H. and Dick, B. 1995. Clinical experiences with the hand-held keratometer. *Klin Monbl Augenheilkd*. **207**: 81–86.

33. Liang, C. L., Hung, K. S., Park, N., Chan, P. and Juo, S. H. J. 2004. Comparison of the handheld Retinomax K-Plus2 and on-table autokeratometers in children with and without cycloplesia. *J Cataract Refract Surg*. **30**: 669–674.

34. Noonan, C. P., Mackenzie, J. and Chandna, A. 1998. Repeatability of the hand-held Nidek auto-keratometer in children. *J AAPOS*. **2**: 186–187.

35. Elawad, H. M. E. A. and Elawad, M. E. A. 2015. Biometric measurements: average intra-ocular lens power for Sudanese patients with senile cataract. *Optics*. **4**: 25–30.

36. Alario, A. F. and Pirie, C. G. 2013. A spectral-domain optical coherence tomography device provides reliable pachymetry measurements in canine eyes. *Vet Rec*. **172**: 605. doi: 10.1136/vr.101530.

37. Alario, A. F. and Pirie, C. G. 2014. Reliability of manual measurements of corneal thickness obtained from healthy canine eyes using spectral-domain optical coherence tomography (SD-OCT). *Can J Vet Res*. **78**: 221–225.

38. Alario, A. F. and Pirie, C. G. 2014. Central corneal thickness measurements in normal dogs: a comparison between ultrasound pachymetry and optical coherence tomography. *Vet Ophthalmol*. **17**: 207–211.

39. Strom, A. R., Cortes, D. E., Rasmussen, C. A., Thomasy, S. M., McIntyre, K., Lee, S. F., Kass, P. H., Mannis, M. J. and Murphy, C. J. 2016. In vivo evaluation of the cornea and conjunctiva of the

normal laboratory beagle using time- and Fourier-domain optical coherence tomography and ultrasound pachymetry. *Vet Ophthalmol*. **19**: 50–56.

40. Wolfel, A. E., Pederson, S. L., Cleymaet, A. M., Hess, A. M. and Freeman, K. S. 2018. Canine central corneal thickness measurements via Pentacam-HR®, optical coherence tomography (Optovue iVue®), and high-resolution ultrasound biomicroscopy. *Vet Ophthalmol*. **21**: 362–370.

41. Alario, A. F. and Pirie, C. G. 2013. Intra and inter-user reliability of central corneal thickness measurements obtained in healthy feline eyes using a portable spectral-domain optical coherence tomography device. *Vet Ophthalmol*. **16**: 446–450.

42. Cleymaet, A. M., Hess, A. M. and Freeman, K. S. 2016. Comparison between Pentacam-HR and optical coherence tomography central corneal thickness measurements in healthy feline eyes. *Vet Ophthalmol*. **19**: 105–114.

43. Pirie, C. G., Alario, A. F., Barysauskas, C. M., Gradil, C. and Uricchio, C. K. 2014. Manual corneal thickness measurements of healthy equine eyes using a portable spectral-domain optical coherence tomography device. *Equine Vet J*. **46**: 631–634.

44. Pinto, N. I. and Gilger, B. C. 2014. Spectral-domain optical coherence tomography evaluation of the cornea, retina, and optic nerve in normal horses. *Vet Ophthalmol*. **17**: 140–148.

45. Famose, F. 2014. Assessment of the use of spectral domain optical coherence tomography (SD-OCT) for evaluation of the healthy and pathological cornea in dogs and cats. *Vet Ophthalmol*. **17**: 12–22.

46. Rival, F., Linsart, A., Isard, P. F., Besson, C. and Dulaurent, T. 2015. Anterior segment

    morphology and morphometry in selected reptile species using optical coherence tomography.

    Vet Ophthalmol. **18**: 53–60.

47. Almazan, A., Tsai, S., Miller, P. E., Lee, S. S., Vilupuru, A. S., Burke, J. A. and Robinson, M. R.

    2013. Iridocorneal angle measurements in mammalian species: normative data by optical

    coherence tomography. *Vet Ophthalmol*. **16**: 163–166.

48. Bland, J. M. and Altman, D. G. 1986. Statistical methods for assessing agreement between two

    methods of clinical measurement, *Lancet*. **327**: 307–310.

49. Lee, B. W., Feuer, W. J., Pouyeh, B., Pelletier, J. S., Vaddavalli, P. K., Lemelman, B. T., See, C.

    and Yoo, S. H. 2013. Agreement between Pentacam and IOLMaster in patients undergoing toric

    IOL implantation. *J Refract Surg*. **23**: 114–120.

50. Lam, A. K. C., Chan, R. and Chiu, R. 2004. Effect of posture and artificial tear on corneal power

    measurements with a handheld automated keratometer. *J Cataract Refract Surg.* **30**: 645–652.

51. Dehnavi, Z., Khabazkhoob, M., Mirzajani, A., Jabbarvand, M., Yekta, A. and Jafarzadehpur, E.

    2015. Comparison of the corneal power measurements with the TMS4-topographer, Pentacam

    HR, IOL Master, and Javal keratometer. *Middle East Afr J Ophthalmol*. **22**: 233–237.

52. Hashemi, H., Aagri, S., Miraftab, M., Emamian, M. H., Shariati, M. and Fotouhi, A. 2014.

    Agreement study of keratometric values measured by Biograph/LENSTAR,

    auto-kerato-refractometer and Pentacam: decision for IOL calculation. *Clin Exp Optom*. **97**:

    450–455.

53. Karabatsas, C. H., Cook, S. D., Powell, K. and Sparrow, J. M. 1998. Comparison of keratometry and videokeratography after penetrating keratoplasty. *J Refract Surg*. **14**: 420–426.

54. Mehravaran, S., Asgari, S., Bigdeli, S., Shahnazi, A. and Hashemi, H. 2014. Keratometry with five different techniques: a study of device repeatability and inter-device agreement. *Int Ophthalmol*. **34**: 869–875.

55. Cho, Y. J., Lim, T. H., Choi, K. Y. and Cho, B. J. 2018. Comparison of ocular biometry using new swept-source optical coherence tomography-based optical biometer with other devices. *Korean J Ophthalmol*. **32**: 257–264.

56. Pulaski, P., Farrer, S., Hamrick, D., Raymond, T. D. and Neal, D. R. 2014. Comparison of ophthalmic model eye radius of curvature using swept source optical coherence tomography and corneal topography. In: ARVO Annual Meeting Abstract. *Invest Ophthalmol Vis Sci*. **55**: 2478.

57. Shajari, M., Cremonese, C., Petermann, K., Singh, P., Muller, M. and Kohnen, T. 2017. Comparison of axial length, corneal curvature, and anterior chamber depth measurements of 2 recently introduced devices to a known biometer. *Am J Ophthalmol*. **178**: 58–64.

58. Zhang, T., Zhou, Y., Young, C. A., Chen, A., Jin, G. and Zheng, D. 2020. Comparison of a new swept-source anterior segment optical coherence tomography and a Scheimpflug camera for measurement of corneal curvature. *Cornea* **39**: 818–822.

59. Freeman, R. D. 1980. Corneal radius of curvature of the kitten and the cat. *Invest Ophthalmol Vis Sci*. **19**: 306–308.

60. Guillon, M., Lydon, D. P. and Wilson, C. 1986. Corneal topography: a clinical model. *Ophthalmic Physiol Opt*. **6**: 47–56.

61. Read, S. A., Collins, M. J., Carney, L. G. and Franklin, R. J. 2006. The topography of the central and peripheral cornea. *Invest Ophthalmol Vis Sci*. **47**: 1404–1415.

62. Sorbara, L., Maram, J., Fonn, D., Woods, C. and Simpson, T. 2010. Metrics of the normal cornea: anterior segment imaging with the Visante OCT. *Clin Exp Optom*. **93**: 150–156.

63. Miyake, T., Mori, H., Watanabe, Y., Yasuno, Y. and Goto, H. 2008. Measurement of radius of corneal curvature using three dimensional anterior segment optical coherence tomography. In: ARVO Annual Meeting Abstract. *Invest Ophthalmol Vis Sci*. **49**: 1869.

64. Hashemi, H., Khabazkhoob, M., Emamian, M. H., Shariati, M., Yekta, A. and Fotouhi, A. 2015. White-to-white corneal diameter distribution in an adult population. *J Current Ophthalmol*. **27**: 21–24.

65. Rüfer, F., Schröder, A. and Erb, C. 2005. White-to-white corneal diameter: normal values in healthy humans obtained with the Orbscan II topography system. *Cornea*. **24**: 259–261.

66. Rosolen, S. G., Riviere, M. L. K., Laillegrand, S., Gautier, B., Picaud, S. and LeGargasson, J. F. 2012. Use of a combined slit-lamp SD-OCT to obtain anterior and posterior segment images in selected animal species. *Vet Ophthalmol*. **15**: 105–115.

67. Andrade, T. F., Moreno, L. R. D. V., Nasciment, F. F., Passareli, J. V. G. C., Rosa, V. D. S., Santos, T. C. D. S., Brinholi, R. B. B. and Andrade, S. F. 2021. Ocular biometry and ophthalmic parameters of normal eyes in French bulldog healthy dogs. *Adv Anim Vet Sci*. **9**: 438–441.

68. Silva, E. G., Pessoa, G. T., Moura, L. S., Guerra, P. C., Rodrigues, R. P. S., Sousa, F. C. A., Ambrosio, C. E. and Alves, F. R. 2018. Biometric, B-mode and color Doppler ultrasound assessment of eyes in healthy dogs. *Pesq Vet Bras*. **38**: 565–571.

69. Boroffka, S. A. E. B., Voorhout, G., Verburuggen, A. M. and Teske, E. 2006. Intraobserver and interobserver repeatability of ocular biometric measurements obtained by means of B-mode ultrasonography in dogs. *Am J Vet Res*. **67**: 1743–1749.

70. Vali, R. and Razeghi, M. 2019. Comparison of transcorneal and transpalpebral ultrasonographic measurements of the eye in Iranian mix breed dog. *Iran J Vet Surg*. **14**: 91–96.

71. Piotrowiak, I., Kaluzny, B. J., Danek, B., Chwiedacz, A., Sikorski, B. L. and Malukiewics, G. 2014. Spectral optical coherence tomography vs. fluorescein pattern for rigid gas-permeable lens fit. *Med Sci Monit*. **20**: 1137–1141.

72. Wolffsohn, J. S., Tharoo, A. and Lakhlani, N. 2015. Optimal time following fluorescein instillation to evaluate rigid gas permeable contact lens fit. *Contact Lens Anterior Eye*. **38**: 110–114.

73. Wolffsohn, J. S., van der Worp, E. and de Brabander, J. 2013. Consensus on recording of gas permeable contact lens fit. *Contact Lens Anterior Eye*. **36**: 299–303.

74. Modis, L., Szalai, E., Kolozsvari, B., Nemeth, G., Vajas, A. and Berta, A. 2012. Keratometry evaluations with the Pentacam high resolution in comparison with the automated keratometry and conventional corneal topography. *Cornea*. **31**: 36–41.

75. Iyamu, E. and Amiebenomo, O. M. A. 2015. The validity and reliability of the handheld SW-100 autokeratometer. *Afr Vision Eye Health*. **74**: a26. doi: 10.4102/aveh.v74i1.26.

76. Murphy, C. J., Zadnik, K. and Mannis, M. J. 1992. Myopia and refractive error in dogs. *Invest Ophthalmol Vis Sci*. **33**: 2459–2463.

77. Kubai, M. A., Bentley, E., Miller, P. E., Mutti, D. O. and Murphy, C. J. 2008. Refractive states of eyes and association between ametropia and breed in dogs. *Am J Vet Res*. **69**: 946–951.

78. Koch, D. D. 2015. The posterior cornea: hiding in plain sight. *Ophthalmology*. **122**: 1070–1071.

79. Byosier, S. E., Chouinard, P. A., Howell, T. J., and Bennett, P. 2018. What do dogs (*Canis familiaris*) see? A review of vision in dogs and implications for cognition research. *Psychon Bull Rev*. **25**: 1798–1813.

80. Miller, P. E. and Murphy, C. J. 1995. Vision in dogs. *J Am Vet Med Assoc*. **207**: 1623–1634.

81. McGreevy, P., Grassi, T. D. and Harman, A. M. 2004. A strong correlation exists between the distribution of retinal ganglion cells and nose length in the dog. *Brain Behav Evol*. **63**: 13–22.

82. Usui, S., Yasuda, H. and Koketsu, Y. 2016. Characteristics of obese or overweight dogs visiting private Japanese veterinary clinics. *Asian Pac J Trop Biomed*. **6**: 338–343.

83. Featherstone, H. J. and Sansom, J. 2004. Feline corneal sequestra: a review of 64 cases (80 eyes) from 1993 to 2000. *Vet Ophthalmol.* **7**: 213–227.

84. Jegou, J-P. and Tromeur, F. 2015. Superficial keratectomy for chronic corneal ulcers refractory to medical treatment in 36 cats. *Vet Ophthalmol.* **18**: 335–340.

85. La Croix, N. C., Van der Wortdt, A. and Olivero, D. K. 2001. Nonhealing corneal ulcers in cats: 29 cases (1991-1999). *J Am Vet Med Assoc.* **218**: 733–735.

86. McDermott, M. L. and Chandler, J. W. 1989. Therapeutic uses of contact lenses. *Surv Ophthalmol.* **33**: 381–394.

87. Carrington, S. D. and Woodward, E. G. 1984. The topography of the anterior surface of the cat's cornea. *Curr Eye Res.* **3**: 823–826.

88. Das, A., Ramani, C. and Shafiuzama, Md. 2016. Keratometry - A scan and prediction of IOL lens power in felines. *Intas Polivet.* **17**: 436–437.

89. Gilger, B. C., Davidson, M. G. and Colitz, C. M. H. 1998. Experimental implantation of posterior chamber prototype intraocular lenses for the feline eye. *Am J Vet Res.* **59**: 1339–1343.

90. Verneuil, M., Marsot, M. and Ruchon, C. 2019. Anterior segment parameters measured in young healthy cats using a rotating Scheimpflug camera. *Vet Ophthalmol.* **22**: 381–384.

91. Eysteinsson, T., Jonasson, F., Sasaki, H., Arnarsson, A., Sverrisson, T., Sasaki, K., Stefansson, E. and the Reykjavik Eye Study Group. 2002. Central corneal thickness, radius of the corneal curvature and intraocular pressure in normal subjects using non-contact techniques: Reykjavik Eye Study. *Acta Ophthalmol Scand.* **80**: 11–15.

92. Tsong, J. W., Alley, C. L., Persaud, T., Grewal, S., Gaughan, J. and Alley, A. A. 2005. Comparison of corneal curvatures, axial lengths, and intraocular lens powers among different world populations. *Invest Ophthalmol Vis Sci.* **46**: 5613.

93. Zhao, H. X., Zhang, L. and Guan, W. Y. 2015. Difference in normal corneal thickness and curvature between Mongolian and Han nationalities. *Int J Ophthalmol.* **8**: 399–402.

94. Uçakhan, O. Ö., Akbel, V., Bıyıklı, Z. and Kanpolat, A. 2013. Comparison of corneal curvature and anterior chamber depth measurements using the manual keratometer, Lenster LS 900 and the Pentacam. *Middle East Afr J Ophthalmol*. **20**: 201–206.

ABSTRACT IN JAPANESE

　角膜曲率とは角膜の曲がり具合を表し、測定値は角膜曲率半径（mm）として示される。角膜の屈折力や乱視の程度を評価でき、コンタクトレンズ（CL）のフィッティングや眼内レンズ（IOL）度数の決定など、様々な場面で参照される。近年では、犬や猫でも、角膜・水晶体疾患の治療において、CL や IOL が使用される例が増加している。しかしながら、獣医眼科領域では角膜曲率測定はまだ一般的でなく、犬と猫の角膜曲率半径を示した報告は少ない。角膜曲率測定を積極的に行い、動物種や品種毎の特徴を明らかにすることで、症例毎により適切な CL の処方および新たな CL 規格の開発に役立つことが期待される。

　本研究では、本邦で一般的に飼育されている犬と猫の角膜曲率半径および角膜乱視についてシグナルメントとの関連を明らかにすることを主目的とし、家庭飼育個体を対象に横断研究を実施した。既報研究の多くが鎮静下や麻酔下で実施されており、装置間の測定値の互換性や信頼性を評価した研究はほとんどない。そのため、本研究では、前述の横断研究に先立ち、実験動物を用いて次の 3 点についても検討した：①覚醒下における角膜曲率測定の実施可能性、②異なる測定装置による測定値の互換性、③測定値の信頼性。

　第 1 章では、鎮静下および覚醒下で測定した角膜曲率半径を比較し、覚醒下における測定値の信頼性を評価した。実験用ビーグル犬 6 例を対象とし、手持ち式自動角膜計（RKT）と前眼部光干渉断層計（OCT）を使用した。測定は、同日に鎮静下と覚醒下で各 1 回ずつと別日に覚醒下で 1 回の、計 3 回実施した。その結果、同一の測定装置で得られた 3 回の測定値は、鎮静の有無や測定日によらず比較的良好な一致がみられた。この結果から、使用した 2

種類の測定装置では、覚醒下の犬でも安定的に角膜曲率測定が可能であることが示された。

　第2章では、3種類の装置で測定した角膜曲率半径を比較し、装置間の互換性を評価した。実験用ビーグル犬7例を対象とし、RKT、OCT、Bモード超音波画像診断装置（US）を使用した。測定は、角膜中心からの距離が異なる複数の領域（RKT：直径4mm、OCT：4–10mm、US：4–14mm）で行い、OCT および US の測定値を RKT の測定値と比較した。その結果、OCT および US では、測定領域が大きくなるにつれて角膜曲率半径も大きくなる傾向がみられ、各々、直径10mm および 12mm において RKT 測定値と最も近似した。その他の領域における OCT および US 測定値はいずれも、RKT 測定値と比べて有意に異なっていた。この結果から、異なる測定装置あるいは測定領域で測定した角膜曲率半径は必ずしも互換性はなく、結果の解釈には注意が必要であることが示唆された。

　第3章では、フルオレセイン染色液を用いたハード CL のフィッティング所見から推測される真の角膜曲率半径と RKT 測定値を比較し、RKT 測定値の信頼性を評価した。実験用ビーグル犬6例と雑種猫8例を対象とし、RKT 測定の後、様々な規格のレンズ（直径8、10、14 mm・ベースカーブ（BC）8.00–10.00 mm）を装着した。フィッティングが最適となるレンズの BC を各径における真の角膜曲率半径とみなした場合、犬猫ともに、RKT 測定値は直径8–10mm レンズの最適 BC と最も近似し、直径14mm レンズの最適 BC よりも有意に小さかった。この結果から、犬と猫の角膜曲率は一定ではなく、RKT 測定値は直径8–10mm 領域の曲率を最も反映するものである可能性が示唆された。

　第4・5章では、RKT を用いて多様なシグナルメントの犬と猫の角膜曲率測定を行い、角膜曲率半径と角膜乱視の大きさについてシグナルメントによる正常参考値を明らかにした。

鳥取大学農学部附属動物医療センターに来院した症例で、角膜形状に影響を及ぼし得る疾患がない症例を対象とした。その結果、犬 237 例、猫 73 例の測定値を取得した。

第 4 章では、合計 16 犬種について犬種別の角膜曲率測定結果を明示した。一部の犬種間では、測定値に有意差がみられた。一般に、角膜曲率半径と体重の間には正の相関がみられたが、体重に対して角膜曲率半径がやや大きめ、または、小さめの犬種も一部存在した。角膜曲率半径と年齢の間に相関性はみられなかった。これらの結果から、犬の角膜曲率半径を予測するためには年齢よりも体重が有用であることが示されたが、犬種によっては必ずしも体重が最適な指標にはならないことが示唆された。

第 5 章では、性別および年齢群別の猫の角膜曲率測定結果を明示した。角膜曲率半径は、雌に比べて雄の方が、1 歳未満の子猫に比べて 1 歳以上の猫の方が有意に大きかった。1 歳以上の猫では年齢群間で有意差はみられなかった。角膜乱視の大きさは、性別や年齢群間で有意差はみられなかった。体重と年齢に基づく角膜曲率半径および角膜乱視の大きさの予測可能性は、各々41–43%と 3%未満であった。猫の角膜曲率半径を予測するためには、体重だけでなく、性別や年齢も考慮する必要があることが示唆された。

本研究では、実験用犬猫および家庭飼育犬猫の角膜曲率測定を通して、覚醒下でも安定した角膜曲率測定が可能であること、測定装置や測定範囲によって測定値に違いが生じる可能性があること、曲率は角膜辺縁部に向かって増大し、RKT 測定値は直径 8–10mm 領域の曲率を反映している可能性が高いこと、そして、動物種や品種、性別、年齢などの個体背景によって角膜曲率半径が異なることが明らかになった。また、国内飼育個体を代表する主要 16 犬種および雑種猫を中心とする猫の性別・年齢群別の角膜曲率半径および角膜乱視の大きさ

について、その正常参考値を詳細に示すことができた。犬と猫における同様の研究は僅かで、特に、犬種別あるいは猫の性別毎の測定値の違いを示した報告はない。本研究成果は、角膜疾患治療における CL の処方をはじめとする様々な積極的治療介入の場面において、その安全性および有効性の向上に寄与する臨床的意義の大きい知見である。また、犬と猫の視機能について理解を深めるうえでも科学的価値の高い知見である。今後は、品種の幅（特に猫の純血種）を拡げてデータを蓄積するとともに、獣医眼科領域における角膜曲率測定の臨床応用の機会を拡げてゆくことが期待される。